



# Modern technologies for quantum photonics I

## Integrated quantum photonics

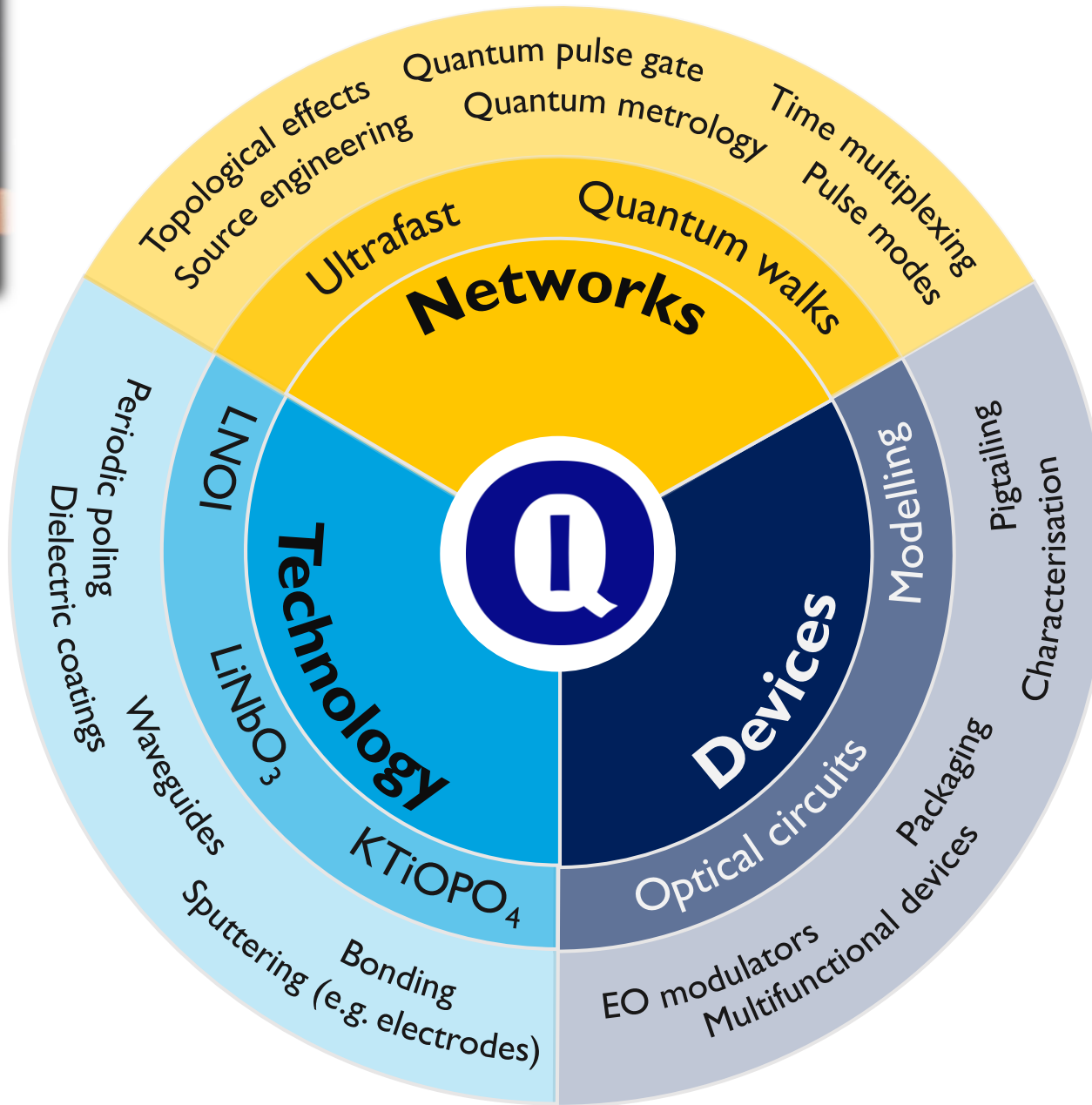
**Benni Brecht**

Christine Silberhorn  
Integrated Quantum Optics  
Paderborn University

ICTP Winter College on Optics:  
Quantum Photonics and Information  
13/02/2020







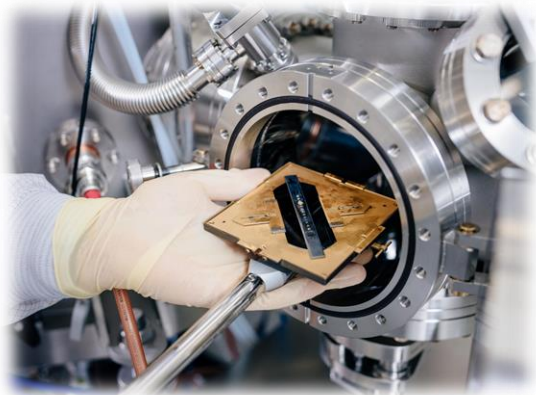
**Christof  
Eigner**



**Harald  
Herrmann**



**Benjamin  
Brecht**





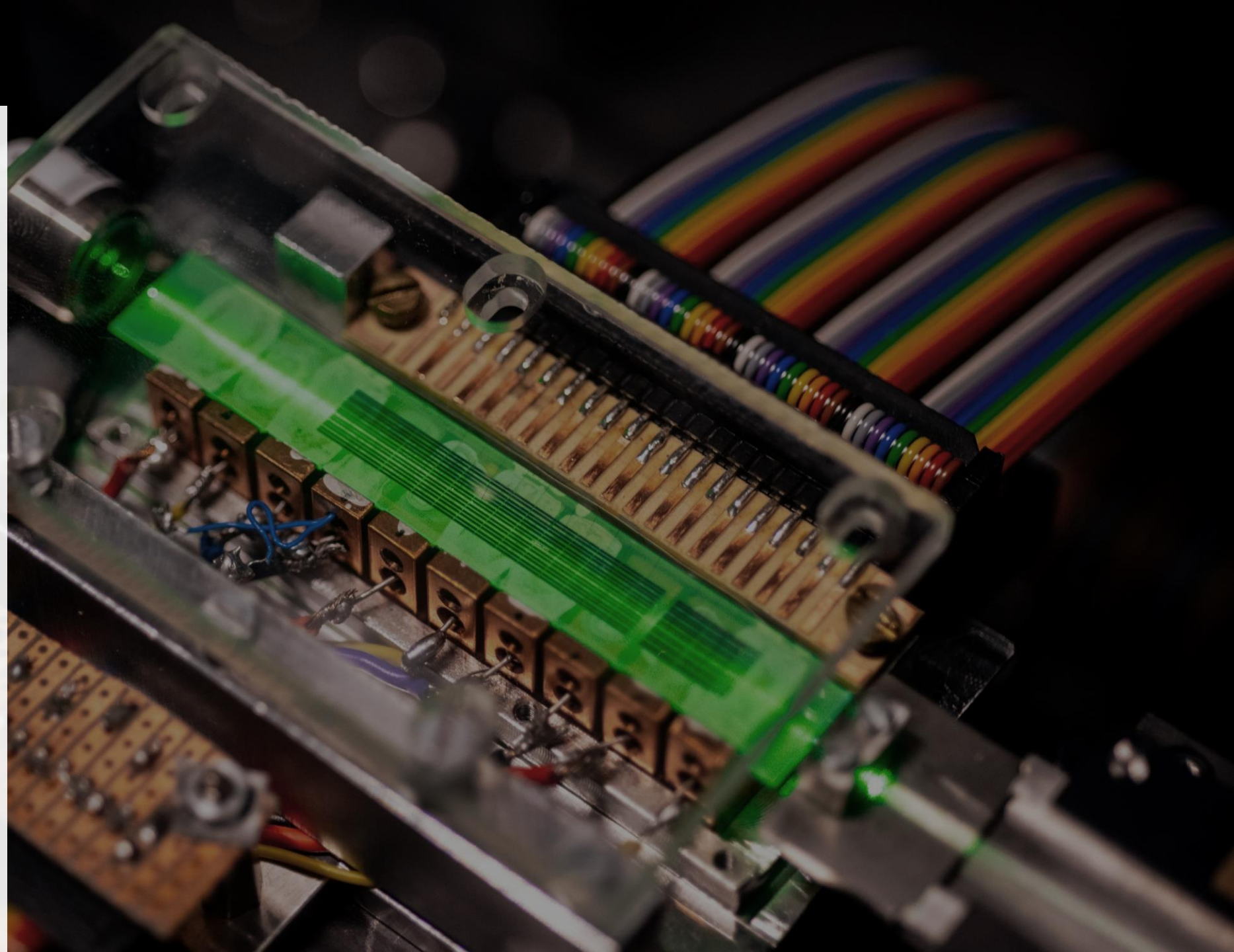
# Outline

Underlying  
concepts

Device  
toolbox

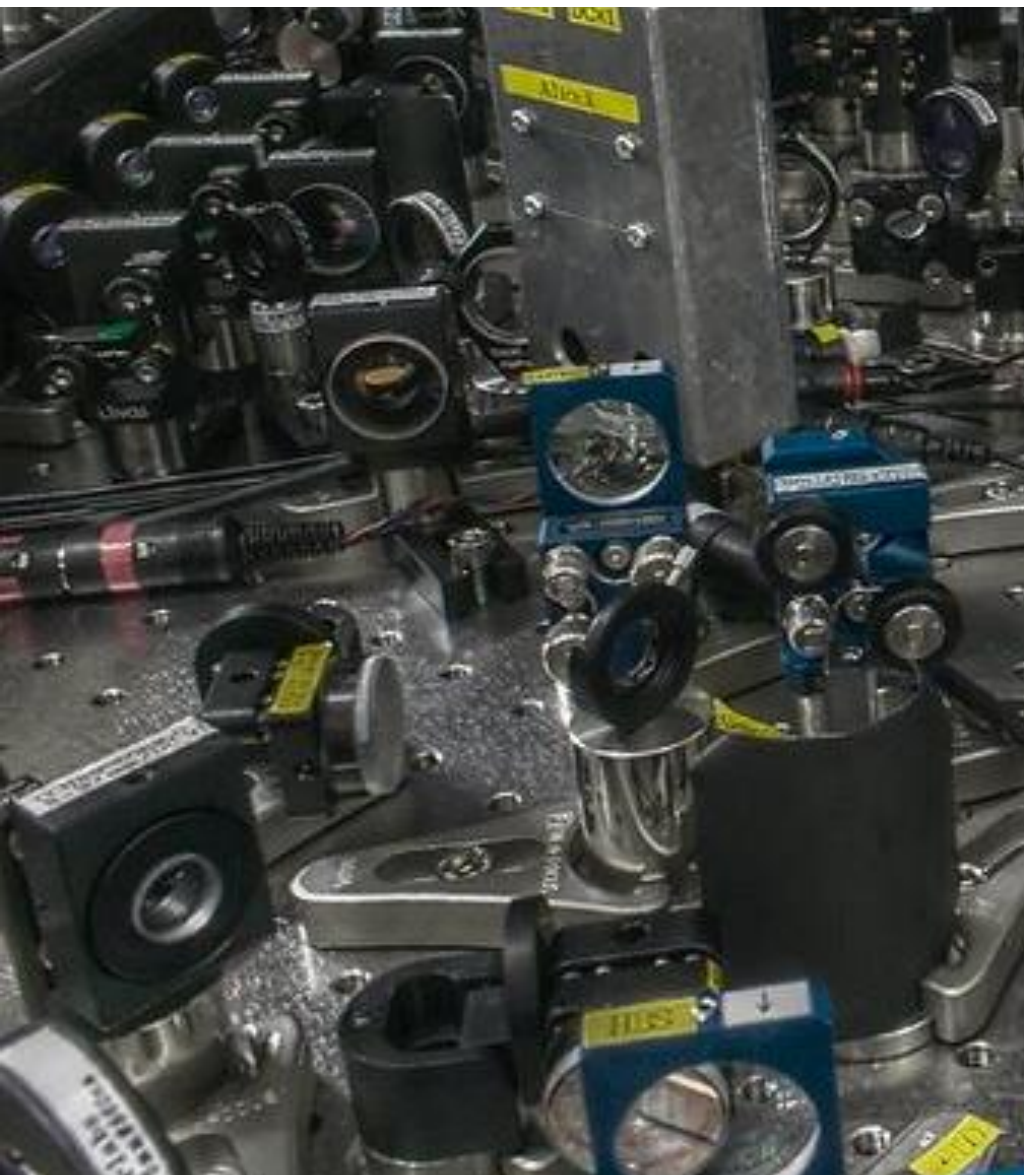
Fabrication  
technology

HOM-on-chip  
circuit

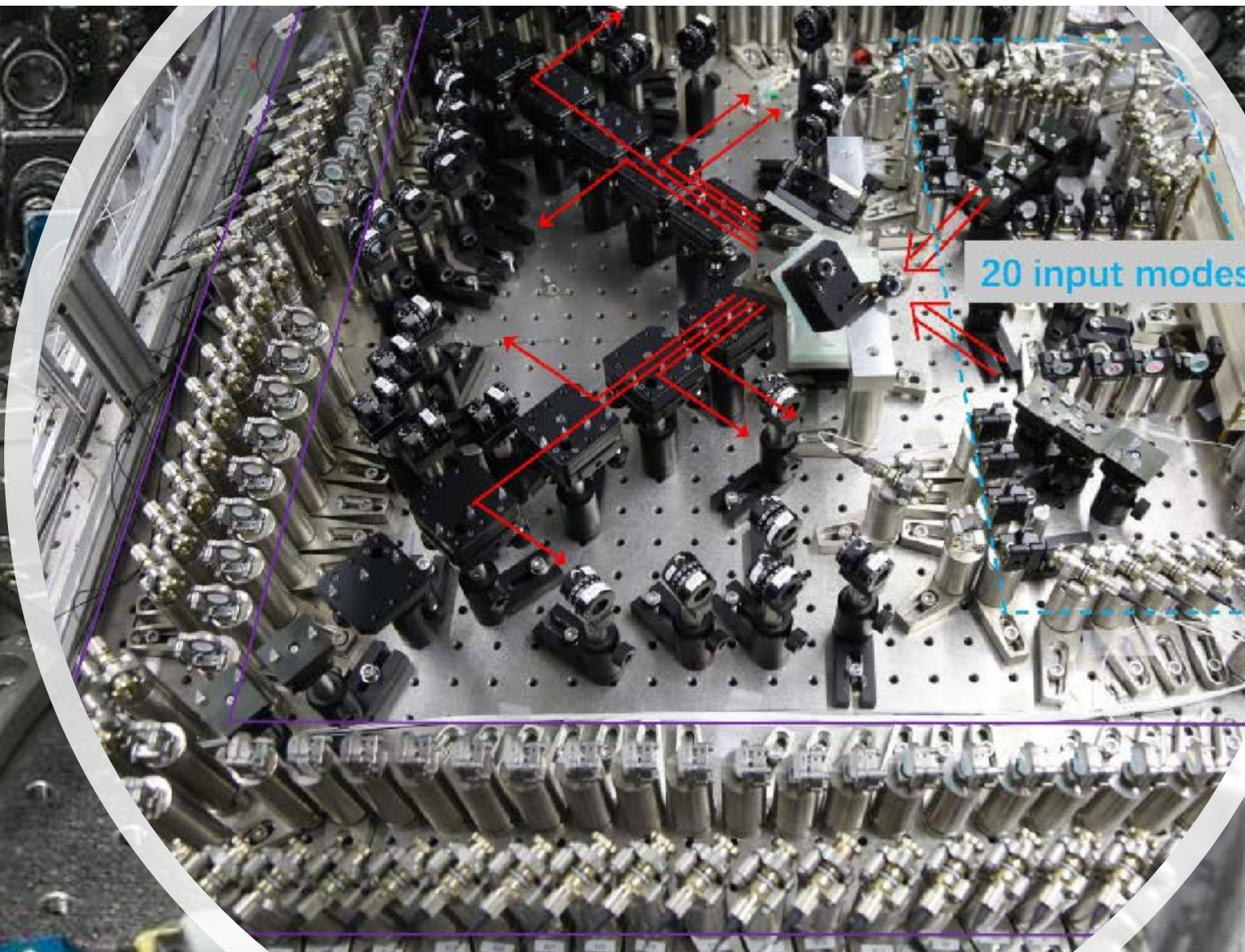




# Why integrated (quantum) photonics?



University of Tokyo, Furusawa group



University of Science and Technology of China, Hefei, Pan group



# History

- ▶ „Invention“ of Integrated Optics by S.E. Miller [1]
- ▶ Roadmap from conventional integrated optics to „Integrated Quantum Optics“ ?

Quantum

## Integrated Optics: An Introduction

By STEWART E. MILLER

(Manuscript received January 29, 1969)

quantum

photon source

quantum

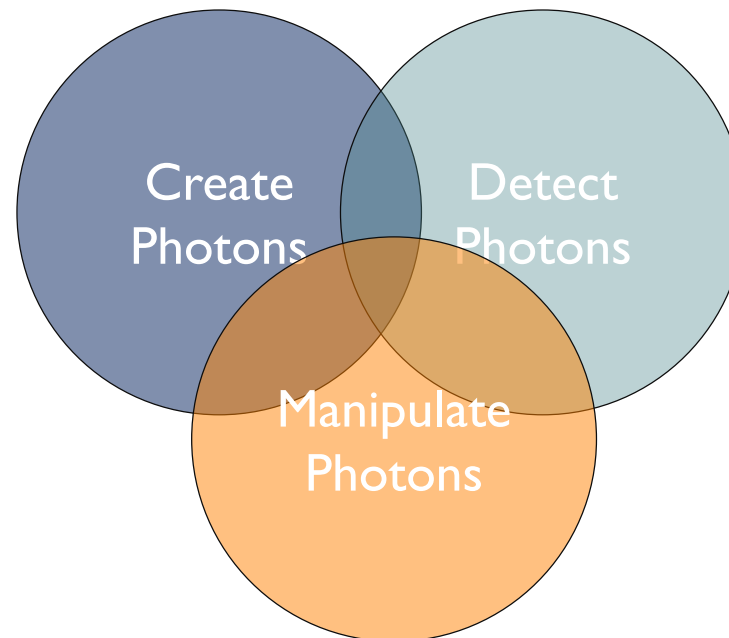
*This paper outlines a proposal for a miniature form of ~~laser beam~~ circuitry. Index of refraction changes of the order of  $10^{-2}$  or  $10^{-3}$  in a substrate such as glass allow guided laser beams of width near 10 microns. Photolithographic techniques may permit simultaneous construction of complex circuit patterns. This paper also indicates possible miniature forms for a ~~laser~~, modulator, and hybrids. If realized, this new art would facilitate isolating the ~~laser~~ circuit assembly from thermal, mechanical, and acoustic ambient changes through small overall size; economy should ultimately result.*



**Keep ideas, but adapt them to quantum optics!**

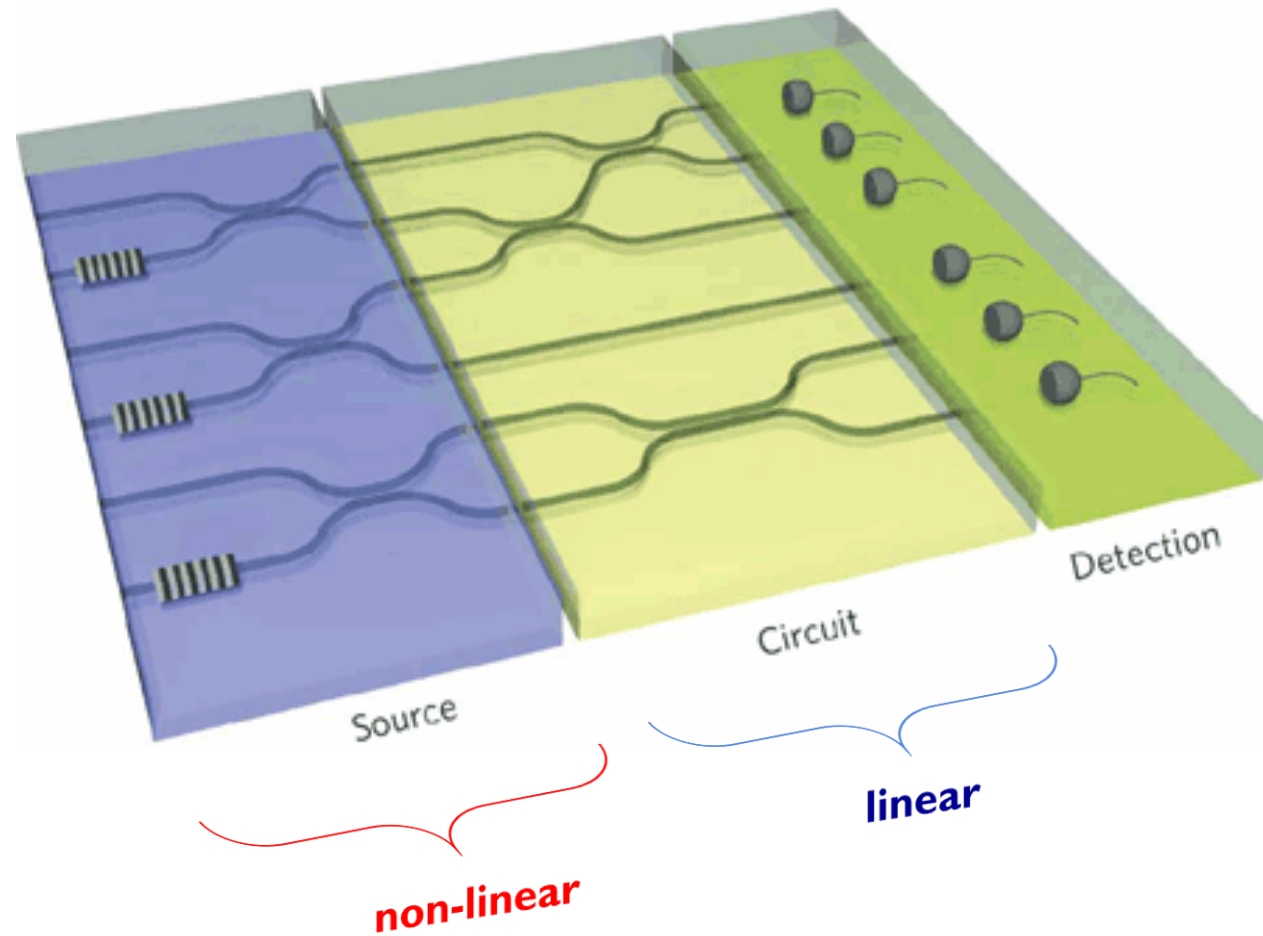
# Quantum optics “on chip”

- ▶ Common structure to all quantum experiments
- ▶ One objective of the Integrated Quantum Optics group:
  - ➔ Integrate as many components as possible (onto a single platform?)



# Integrated quantum photonics

## Photonic quantum simulator



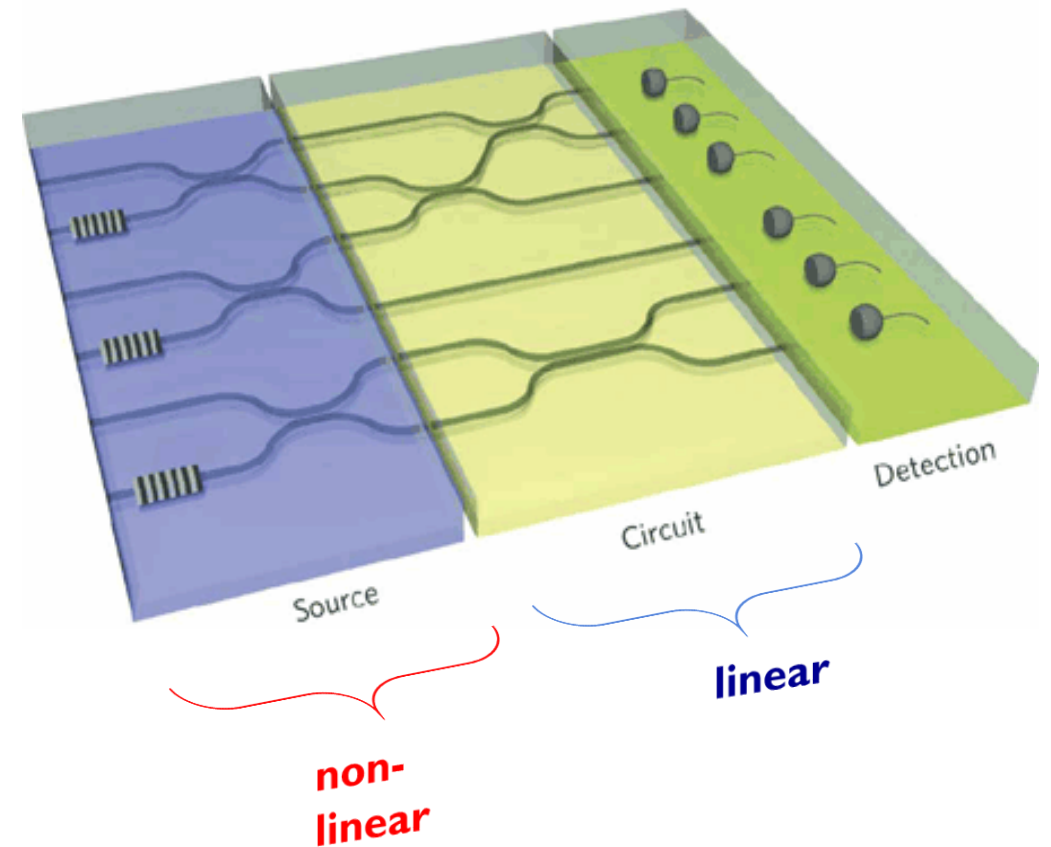


# Integrated quantum photonics

## Photonic quantum simulator

### Advantages:

- Many spatial modes available / controllable
- Interferometric stability of large optical system
- Compact devices; miniaturization
- „Simple“ operation
- High efficiency (?)



## Boson Sampling on a Photonic Chip

Justin B. Spring,<sup>1,\*</sup> Benjamin J. Metcalfe,<sup>1</sup> Peter C. Humphreys,<sup>1</sup> W. Steven Kolthammer,<sup>1</sup> Xian-Min Jin,<sup>1,2</sup> Marco Barbieri,<sup>1</sup> Animesh Datta,<sup>1</sup> Nicholas Thomas-Peter,<sup>1</sup> Nathan K. Langford,<sup>1,3</sup> Dmytro Kundys,<sup>4</sup> James C. Gates,<sup>4</sup> Brian J. Smith,<sup>1</sup> Peter G. R. Smith,<sup>1</sup> Ian A. Walmsley<sup>1,5</sup>

Although universal quantum computers ideally solve problems such as factoring integers exponentially more efficiently than classical machines, the formidable challenges in building such devices motivate the demonstration of simpler, problem-specific algorithms that still promise a quantum speedup. We constructed a quantum boson-sampling machine (QBSM) to sample the output distribution resulting from the nonclassical interference of photons in an integrated photonic circuit, a problem thought to be exponentially hard to solve classically. Unlike universal quantum computation, boson sampling merely requires indistinguishable photons, linear state evolution, and detectors. We benchmarked our QBSM with three and four photons and analyzed sources of sampling inaccuracy. Scaling up to larger devices could offer the first definitive quantum-enhanced computation.

Universal quantum computers require physical systems that are well isolated from the decohering effects of their environment, while at the same time allowing precise manipulation during computation. They also require qubit-specific state initialization, measurement, and generation of quantum correlations across the system (1–4). Although there has been substantial progress in proof-of-principle demonstrations of quantum computation (5–8), simultaneously meeting these demands has proven difficult. This motivates the search for schemes that can demonstrate quantum-enhanced computation under more favorable experimental conditions. Investigating the space between classical and universal quantum computers has attracted broad interest (9–11).

Boson sampling has recently been proposed as a specific quantum computation that is more efficient than its classical counterpart but only requires indistinguishable bosons, low decoherence linear evolution, and measurement (12). The distribution of bosons that have undergone a

unitary transformation  $U$  is thought to be exponentially hard to sample from classically (12). The probability amplitude of obtaining a certain output is directly proportional to the permanent of a corresponding submatrix of  $U$  (13). The permanent expresses the wave function of identical bosons, which are symmetric under exchange (14, 15); in contrast, the Slater determinant expresses the wave function of identical fermions, which are antisymmetric under exchange. Whereas determinants can be evaluated efficiently, permanents have long been believed to be hard to compute (16); the best-known algorithm scales exponentially with the size of the matrix.

One can envision a race between a classical and a quantum machine to sample the boson distribution given an input state and  $U$ . The classical machine would evaluate at least part of the probability distribution, which requires the analysis of matrix permanents. An ideal quantum boson-sampling machine (QBSM) instead creates indistinguishable bosons, physically implements  $U$ , and records the outputs. Although the QBSM is not believed to efficiently estimate any individual matrix permanent, for a sufficiently large system it is expected to beat the classical computer in sampling over the entire distribution (12).

Photonics is a natural platform to implement boson sampling because sources of indistinguishable photons are well developed (17), and integrated optics offers a scalable route to low decoherence linear transformations over many

modes (18). Such circuits can be rapidly reconfigured to sample from a user-defined operation (19, 20). Importantly, boson sampling requires neither nonlinearities nor on-demand entanglement, which are substantial challenges in photonic universal quantum computation (21). This clears the way for experimental boson sampling with existing photonic technology, building on the extensively studied two-photon Hong-Ou-Mandel interference effect (22).

A QBSM (Fig. 1) samples the output distribution of a multiparticle bosonic quantum state  $|\Psi_{\text{in}}\rangle$ , prepared from a specified initial state  $|\mathbf{T}\rangle$  and linear transformation  $\Lambda$ . Unavoidable losses in the system imply  $\Lambda$  will not be unitary, although lossy QBSMs can still surpass classical computation (12, 23). A trial begins with the input state  $|\mathbf{T}\rangle = |T_1, \dots, T_M\rangle \propto \prod_{i=1}^M (a_i^\dagger)^{T_i} |0\rangle$ , which describes  $N = \sum_{i=1}^M T_i$  particles distributed in  $M$  input modes in the occupation-number representation. The output state  $|\Psi_{\text{out}}\rangle$  is generated according to the linear map between input and output mode creation operators  $\hat{a}_i^\dagger = \sum_{j=1}^M \Lambda_{ji} \hat{b}_j^\dagger$ , where  $\Lambda$  is an  $M \times M$  matrix. Lastly, the particles in each of the  $M$  output modes are counted. The

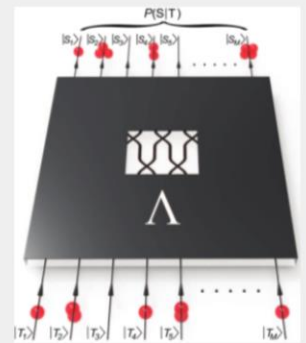


**Fig. 1.** Model of quantum boson sampling. Given a specified initial number state  $|\mathbf{T}\rangle = |T_1, \dots, T_M\rangle$  and linear transformation  $\Lambda$ , a QBSM efficiently samples from the distribution  $P(\mathbf{S}|\mathbf{T})$  of possible outcomes  $|\mathbf{S}\rangle = |S_1, \dots, S_M\rangle$ .

## Waveguide

S  
Rarity, Siyuan Yu, Jeremy L. O'Brien\*

will likely require an integrated optics architecture  $n$ , and scalability. We demonstrate high-fidelity simulations of key quantum photonic circuits, including visibility of  $94.8 \pm 0.5\%$ ; a controlled-NOT gate with  $\pm 0.2\%$ ; and a path-entangled state of two photons  $y$  that it is possible to directly "write" sophisticated chip, which will be of benefit to future quantum information processing, communication, metrology, and science of quantum optics.

Although a number of photonic quantum circuits have been realized for quantum metrology (3, 4, 10–13), lithography (6), quantum logic gates (14–20), and other entangling circuits (21–23), these demonstrations have relied on large-scale (bulk) optical elements bolted to large optical tables, thereby making them inherently unscalable.

We demonstrate photonic quantum circuits using silica waveguides on a silicon chip. The monolithic nature of these devices means that the correct phase can be stably realized in what would otherwise be an unstable interferometer, greatly simplifying the task of implementing sophisticated photonic quantum circuits. We fabricated hundreds of devices on a single wafer and find that performance across the devices is robust, repeatable, and well understood.

A typical photonic quantum circuit takes several optical paths or modes (some with photons, some without) and mixes them together in a linear optical network, which in general con-

## ARTICLES

PUBLISHED ONLINE: 3 MARCH 2013 | DOI: 10.1038/NPHOTON.2013.26

nature  
photonics

## Anderson localization of entangled photons in an integrated quantum walk

Andrea Crespi<sup>1,2</sup>, Roberto Osellame<sup>1,2,\*</sup>, Roberta Ramponi<sup>1,2</sup>, Vittorio Giovannetti<sup>3</sup>, Rosario Fazio<sup>3,4</sup>, Linda Sansoni<sup>5</sup>, Francesco De Nicola<sup>5</sup>, Fabio Sciarrino<sup>5,6,\*</sup> and Paolo Mataloni<sup>5,6</sup>

First predicted for quantum particles in the presence of a disordered potential, Anderson localization is a ubiquitous effect, observed also in classical systems, arising from the destructive interference of waves propagating in static disordered media. Here we report the observation of this phenomenon for pairs of polarization-entangled photons in a discrete quantum walk affected by position-dependent disorder. By exploiting polarization entanglement of photons to simulate different quantum statistics, we experimentally investigate the interplay between the Anderson localization mechanism and the bosonic/fermionic symmetry of the wavefunction. The disordered lattice is realized by an integrated array of interferometers fabricated in glass by femtosecond laser writing. A novel technique is used to introduce a controlled phase shift into each unit mesh of the network. This approach yields great potential for quantum simulation and for implementing a computational power beyond the one of a classical computer in the 'hard-to-simulate' scenario.

In 1958, P.W. Anderson<sup>1</sup> predicted that the wavefunction of a quantum particle can be localized in the presence of a static disordered potential. As a consequence, it is expected that particle and energy transport through a disordered medium should be strongly suppressed and that an initially localized wave packet should not spread out with time. More than 50 years after its discovery, Anderson localization is still widely studied and it has pervaded many different areas of physics ranging from condensed matter and cold atoms to wave dynamics and quantum chaos<sup>2</sup>.

This phenomenon emerges quite generically in the behaviour of waves in complex media, and it has been experimentally observed in a variety of different systems, including Bose-Einstein condensates<sup>3,4</sup>, light in semiconductor powders<sup>5</sup>, inverted opals<sup>6</sup> and photonic lattices<sup>7–9</sup>, single photons in bulk optics<sup>10</sup> and fibre loops<sup>11</sup>, microwaves in strongly scattering samples<sup>12</sup>, as well as ultrasound waves in a three-dimensional elastic system<sup>13</sup>. Anderson localization arises from destructive interference among different scattering paths of a quantum particle propagating in a static disordered medium. As such, it is intrinsically a single-particle effect. However, when multiple particles co-propagate in the same medium, quantum correlations, present in the initial state or induced by the quantum statistics of the involved particles, may influence the overall wavefunction evolution in a way that is not dissimilar from the bunching/antibunching mechanisms observed in interferometric experiments<sup>14–17</sup>. Such sensitivity to quantum correlations is not related to the presence of interactions between the co-propagating walkers.

Therefore, a direct interaction between the walkers should be avoided in order to investigate the pure effect of quantum correlations. In this work we experimentally study the localization properties of a pair of non-interacting particles obeying bosonic/fermionic statistics<sup>18</sup> by simulating a one-dimensional quantum walk (QW) of two-photon polarization-entangled state in a disordered medium. To implement different quantum statistics we exploit a formal mapping, developed in ref. 14, which links the symmetry

of the polarization-entangled biphoton input state to the bosonic/fermionic symmetry of the wavefunction of two particles. The experimental investigation of these complex interference effects is enabled by the perfect phase stability provided by miniaturized integrated waveguide circuits<sup>19</sup>. After briefly reviewing some basic concepts about QWs, we will detail the peculiarities of our experimental implementation, reserving the second part of the Article to the discussion of the observed results.

### One-dimensional quantum walks

A one-dimensional QW<sup>20</sup> is an extension of the classical random walk, where the walker goes back and forth along a line and the direction at each step depends on the result of a fair coin flip. At the quantum level, interference and superposition phenomena lead to a non-classical behaviour of the walker, giving rise to new interesting effects that can be harnessed to exponentially speed up search algorithms<sup>21</sup> and to realize universal quantum computation<sup>22</sup>. QWs have also been proposed to analyse energy transport in biological systems<sup>23,24</sup>. Different experimental implementations of single-particle QWs have been demonstrated with trapped atoms<sup>25,26</sup>, ions<sup>27</sup>, energy levels in NMR schemes<sup>28</sup>, photons in waveguide structures<sup>29</sup>, in bulk optics<sup>10,30</sup>, and in a fibre loop configuration<sup>11,31</sup>. Very recently, QWs of two identical photons have been demonstrated, but only in ordered structures<sup>19,32,33</sup>.

A physical realization of a one-dimensional discrete QW can be provided by photons passing through a cascade of balanced beam splitters arranged in a network of Mach-Zehnder interferometers, as represented conceptually in Fig. 1. Each beam splitter simultaneously implements the quantum coin operation (that is, the choice of direction in which the particle will move) and the step operator, which shifts the walker in the direction fixed by the quantum coin state. The time evolution is simulated stroboscopically<sup>19</sup>. Accordingly, every output of a beam splitter of the network corresponds to a given point in the space-time of the QW, with the

<sup>1</sup>Istituto di Fotonica e Nanotecnologie, Consiglio Nazionale delle Ricerche (IFN-CNR), Piazza Leonardo da Vinci, 32, I-20133 Milano, Italy. <sup>2</sup>Dipartimento di Fisica, Politecnico di Milano, Piazza Leonardo da Vinci, 32, I-20133 Milano, Italy. <sup>3</sup>NIST, Scuola Normale Superiore and Istituto di Nanoscienze - CNR, I-56126 Pisa, Italy. <sup>4</sup>Center for Quantum Technologies, National University of Singapore, 117542 Singapore, Singapore. <sup>5</sup>Dipartimento di Fisica, Sapienza Università di Roma, Piazzale Aldo Moro, 5, I-00185 Roma, Italy. <sup>6</sup>Istituto Nazionale di Ottica, Consiglio Nazionale delle Ricerche (INO-CNR), Largo Enrico Fermi, 6, I-50125 Firenze, Italy. \*e-mail: roberto.osellame@polimi.it; fabio.sciarrino@unroma1.it

322

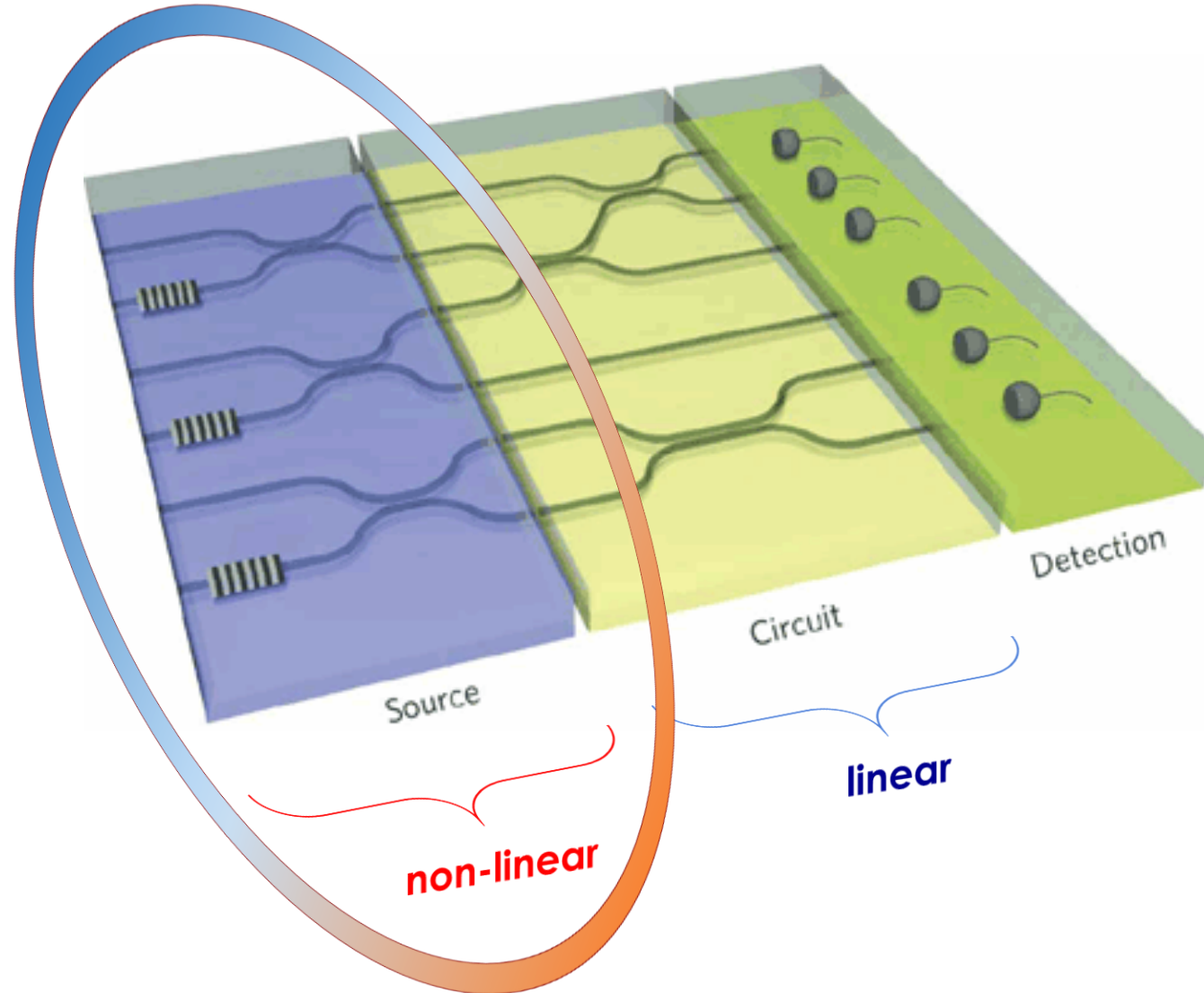
NATURE PHOTONICS | VOL 7 | APRIL 2013 | www.nature.com/naturephotonics





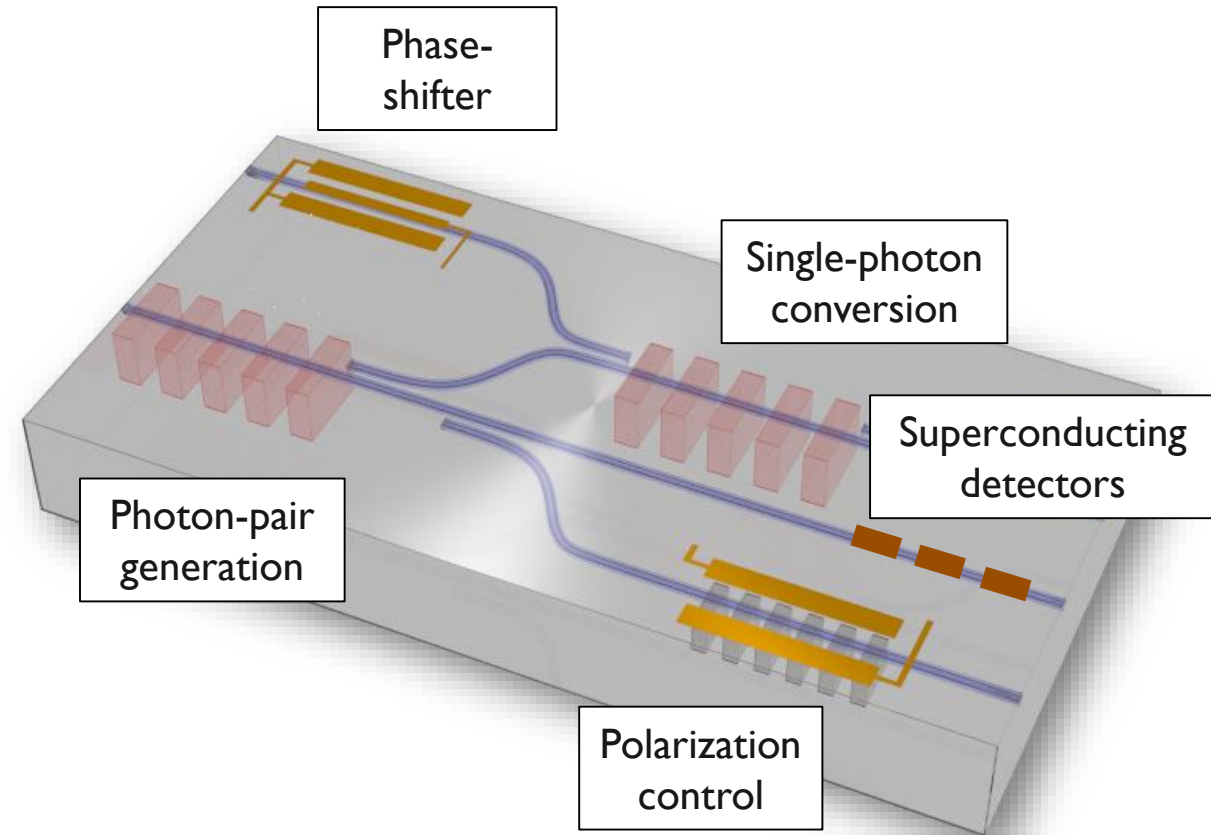
# Integrated quantum photonics

## Photonic quantum simulator



# We chose: lithium niobate

- **minimized decoherence**  
✓ low-loss waveguides
- **stability and scalability**  
✓ integrated devices
- **photon-pair generation**  
✓  $\chi^{(2)}$  nonlinearity
- **fast photon routing**  
✓ fast electro-optic switches



Implementation of **complex quantum circuits** in LN



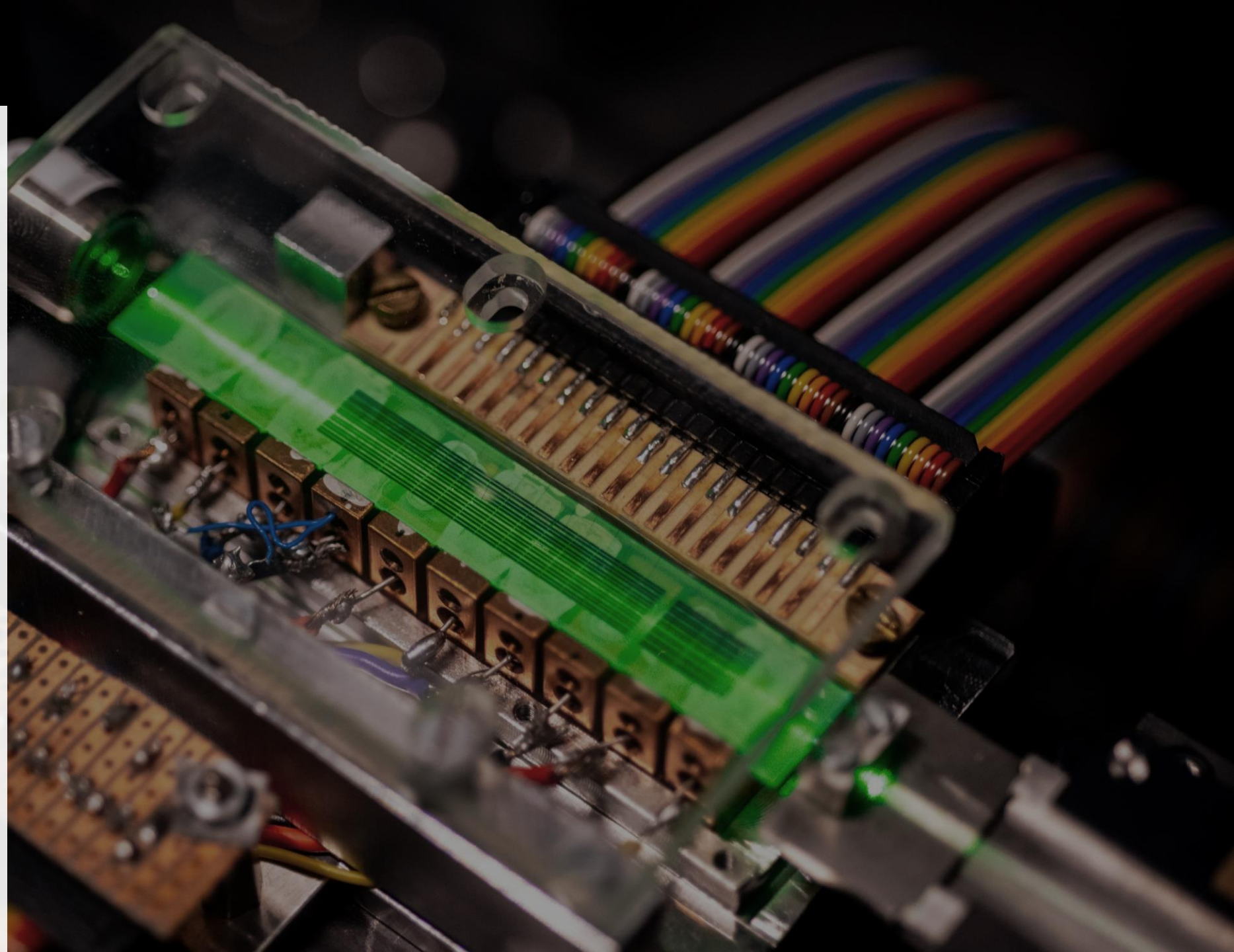
# Outline

Underlying  
concepts

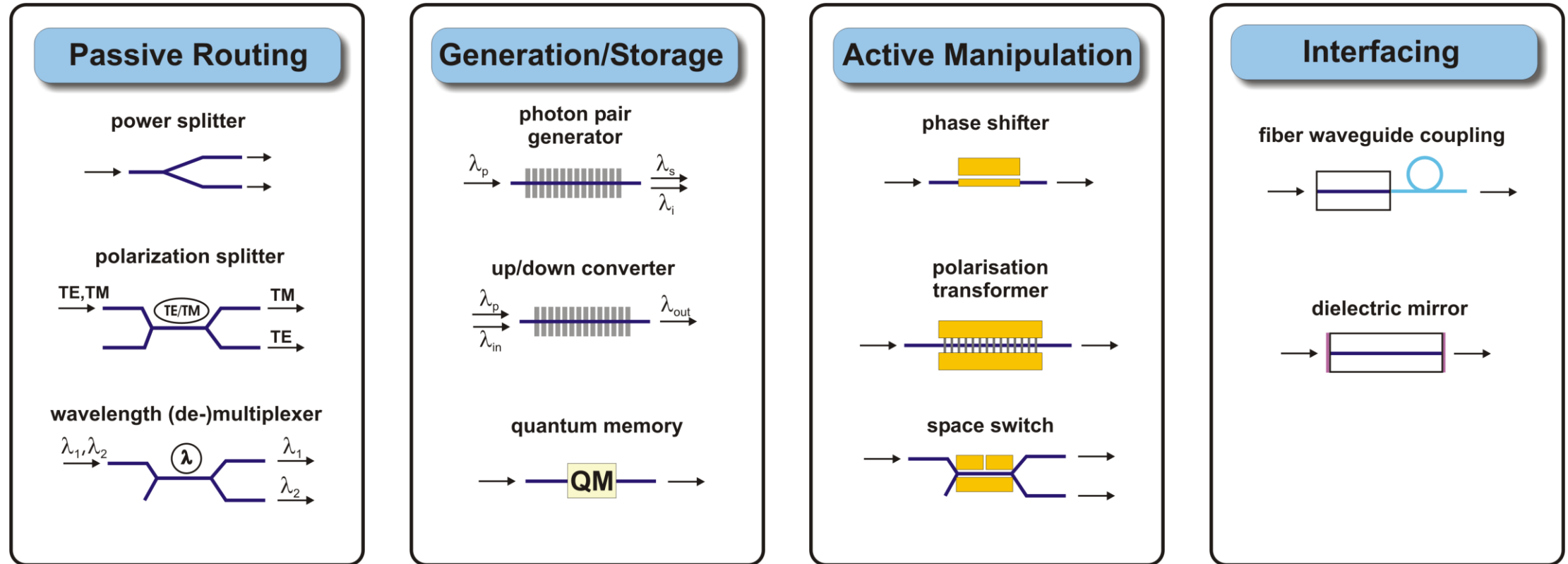
**Device  
toolbox**

Fabrication  
technology

HOM-on-chip  
circuit



# Components for integrated quantum circuits

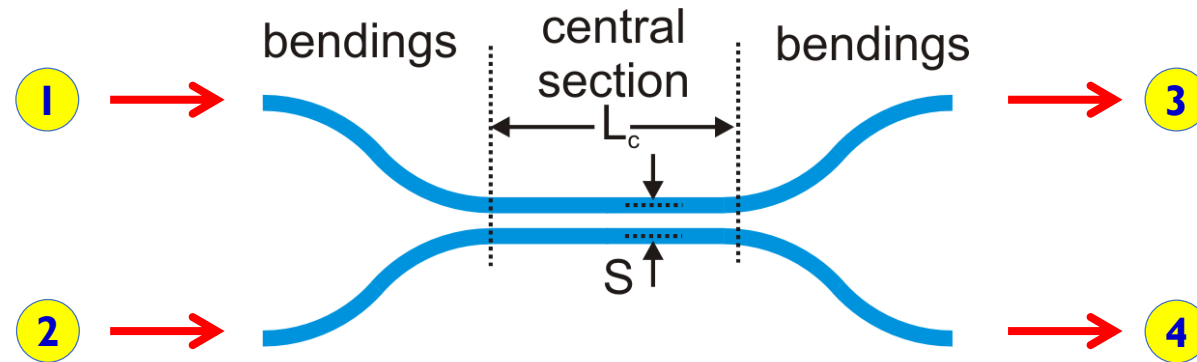


Every single of these components has already been developed and optimized for classical optical applications (telecomms, sensing), but

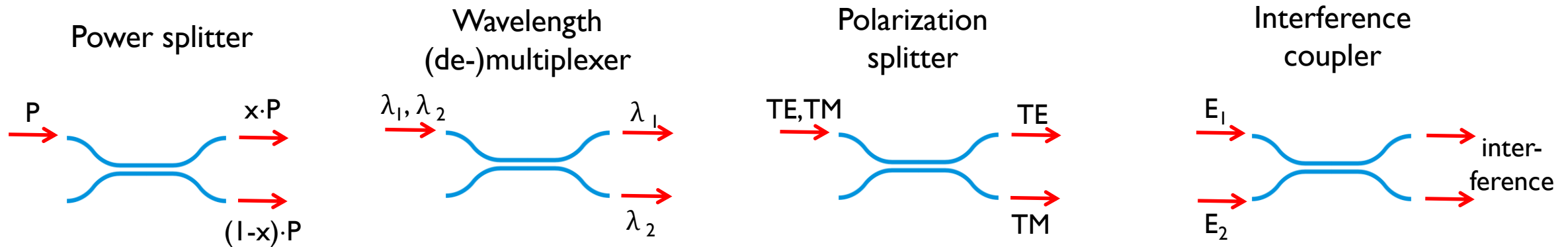
**Re-design / optimization for quantum applications is required.**

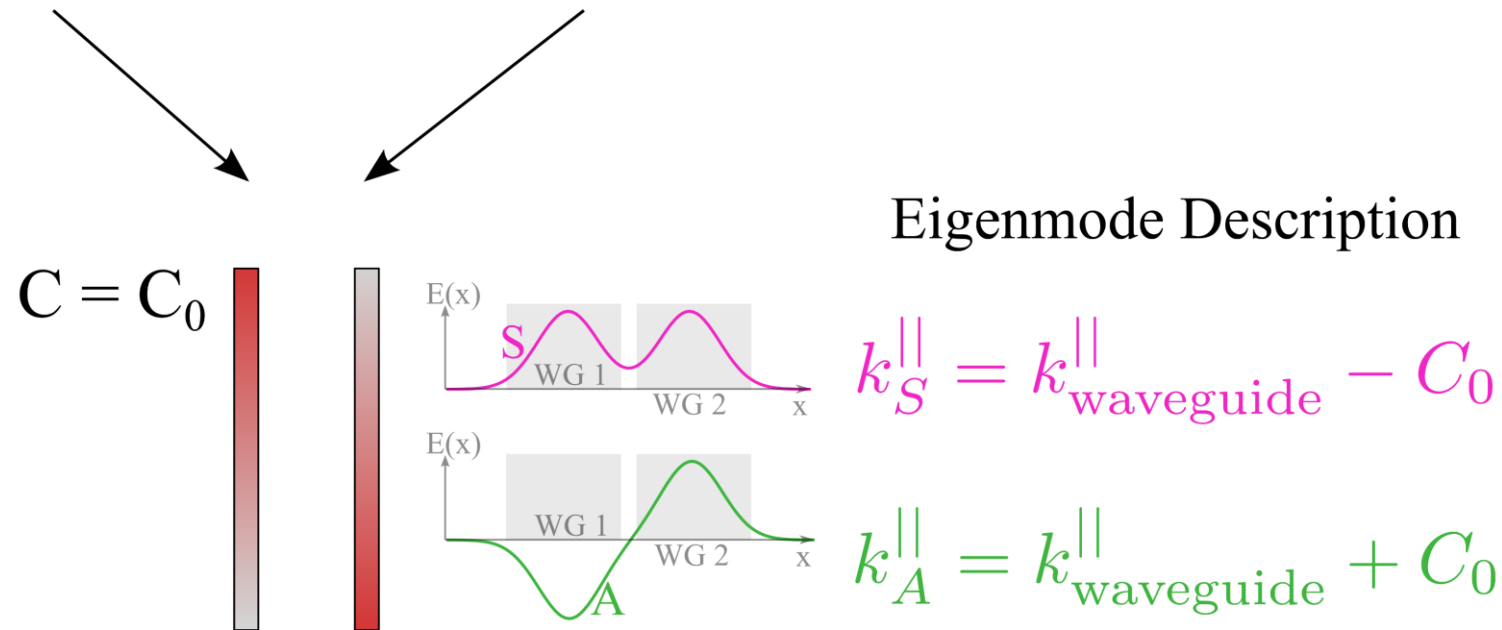
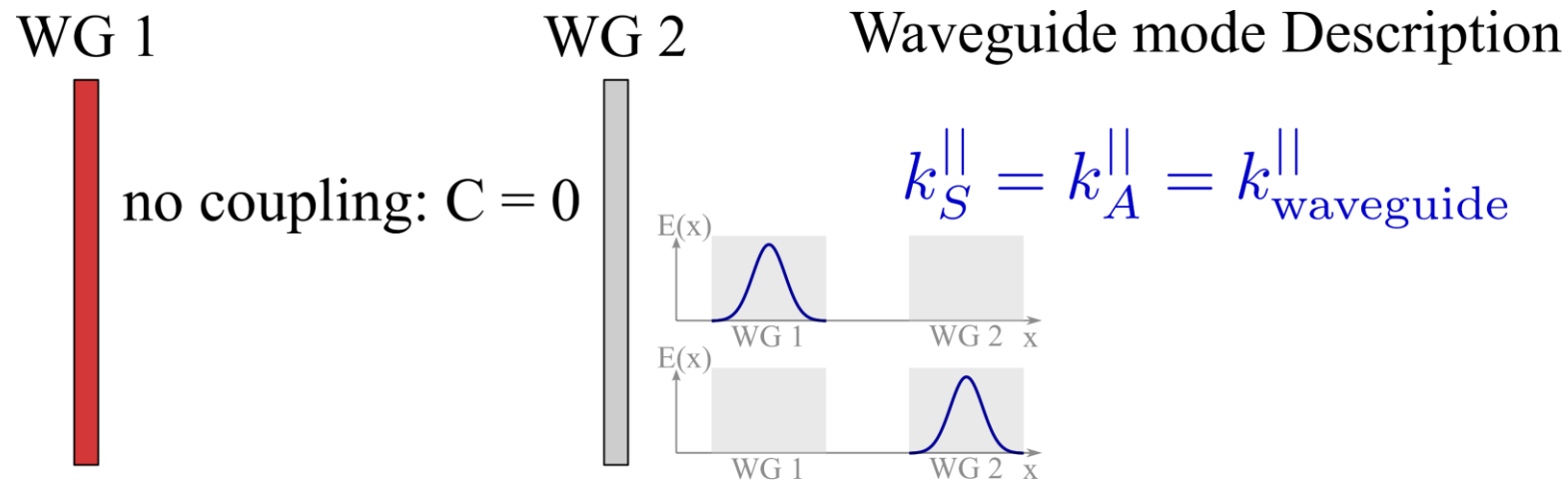


# Passive routing – directional couplers



## Example applications:

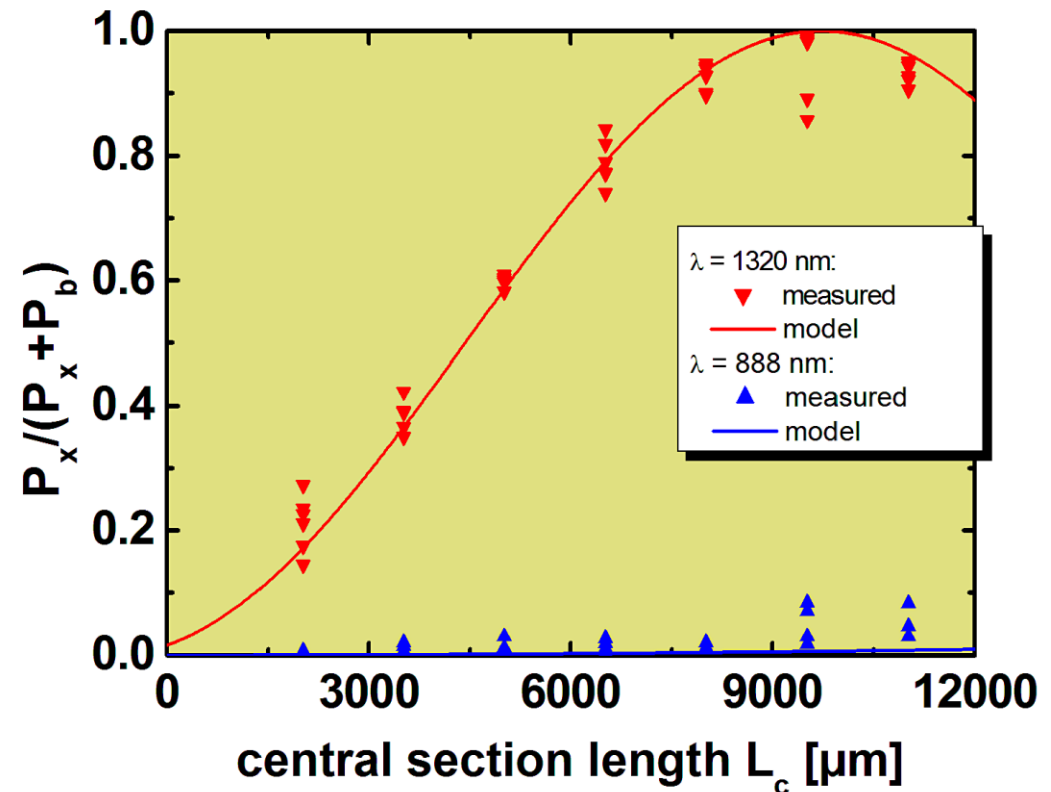
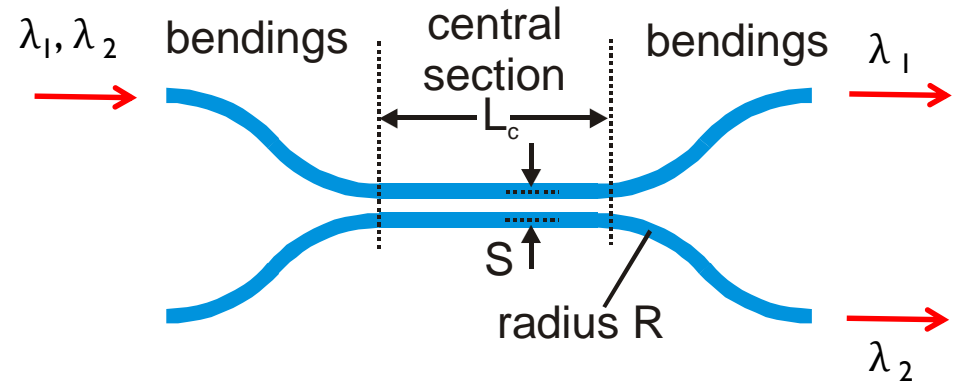






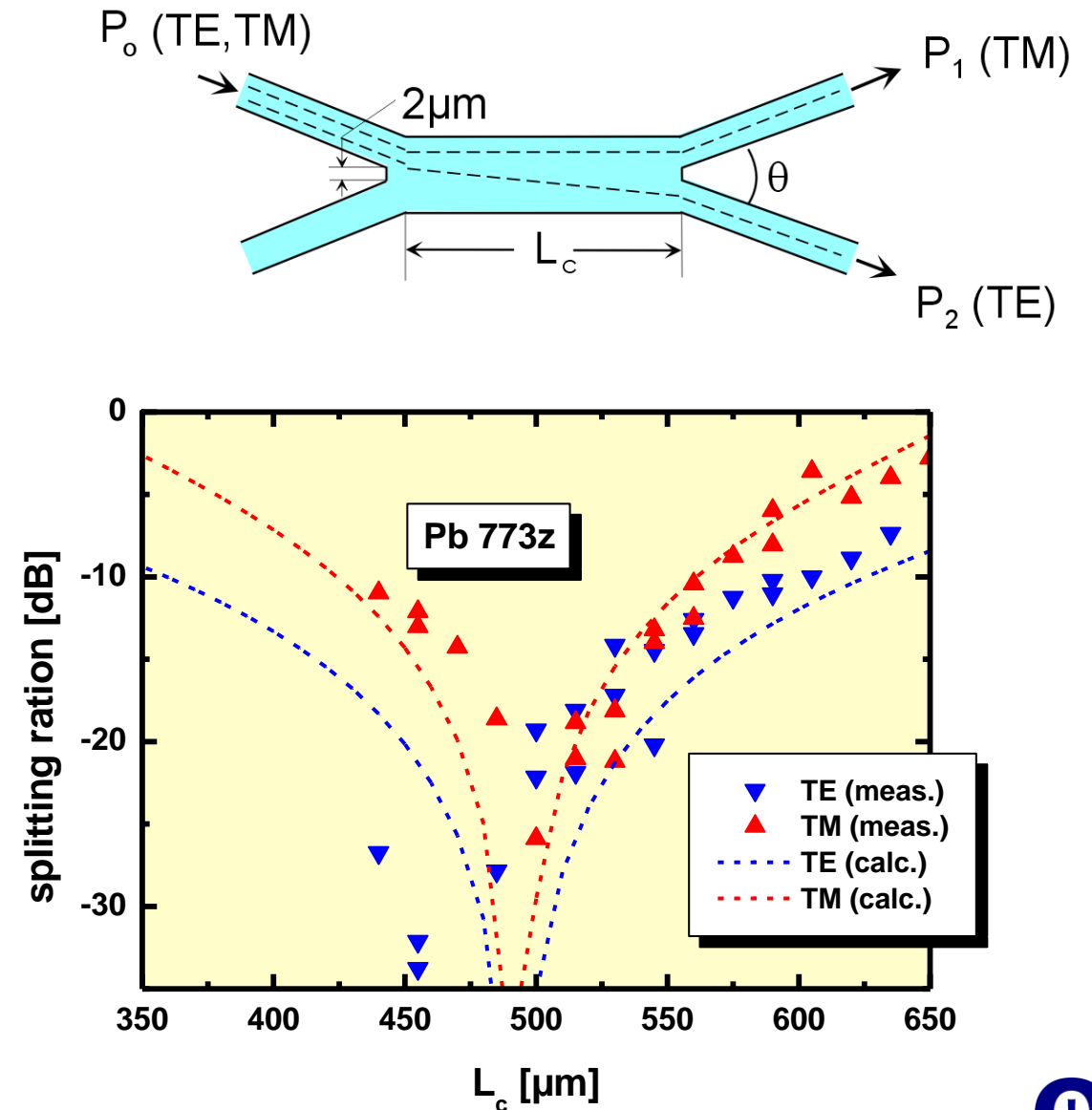
# Example I – wavelength demultiplexer

- ▶ Wavelength division demultiplexer to separate 890 nm from 1320 nm (TM-polarization):
- ▶ Weak coupling structure with large separation provides cross-coupling at the longer wavelength and (almost) no coupling at short wavelength
- ▶ Splitting ratios  $> 15$  dB can be obtained for couplers with  $L_c \approx 9000 \dots 11000 \mu\text{m}$



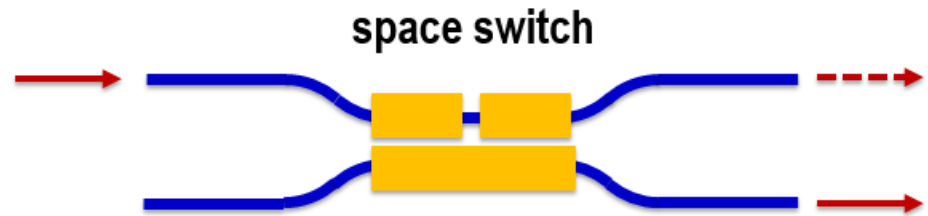
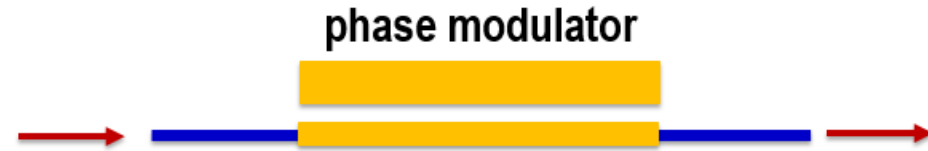
## Example 2 – polarization splitter

- ▶ Zero-gap directional coupler acting as polarization splitter at 1550 nm
- ▶ Low coupling order provides robust and wavelength independent operation
- ▶ Experimental results:
  - ▶ splitting ratios  $\approx 20$  dB achieved for central section length  $L_c = 480 \mu\text{m}$
  - ▶ excess loss typically below 0.5 dB





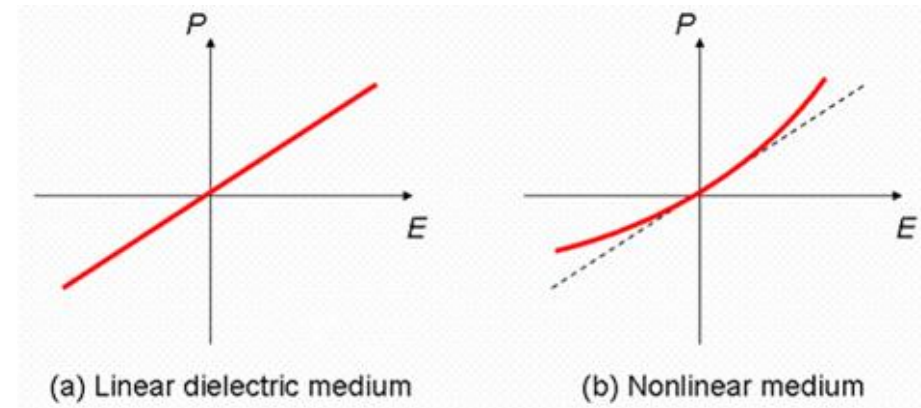
# Active manipulation – electro-optic modulators



requires  $\chi^{(2)}$  nonlinearity!

# Nonlinear optical polarization

- Nonlinearity in the dielectric polarization



$$\vec{P}(\vec{r}, t) = \epsilon_0 \chi(\vec{r}, t) \vec{E}(\vec{r}, t) \quad \vec{P}(\vec{r}, t) = \epsilon_0 \chi(\vec{r}, t, \vec{E}) \vec{E}(\vec{r}, t)$$

- Nonlinear polarization is the driving source for the generation of waves at new frequencies

non centrosymmetric crystal required

- Taylor expansion of nonlinear polarization

$$\vec{P} = \epsilon_0 (\chi^{(1)} \cdot \vec{E} + \chi^{(2)} : \vec{E} \vec{E} + \chi^{(3)} : \vec{E} \vec{E} \vec{E} + \dots)$$

electro-optic manipulation: optical & electric fields



# Electro-optic modulation

- Phase modulation via an externally applied voltage

- local change of the refractive index

$$\Delta n(x, y) = \frac{1}{2} n_e^3 r_{33} E_y(x, y)$$

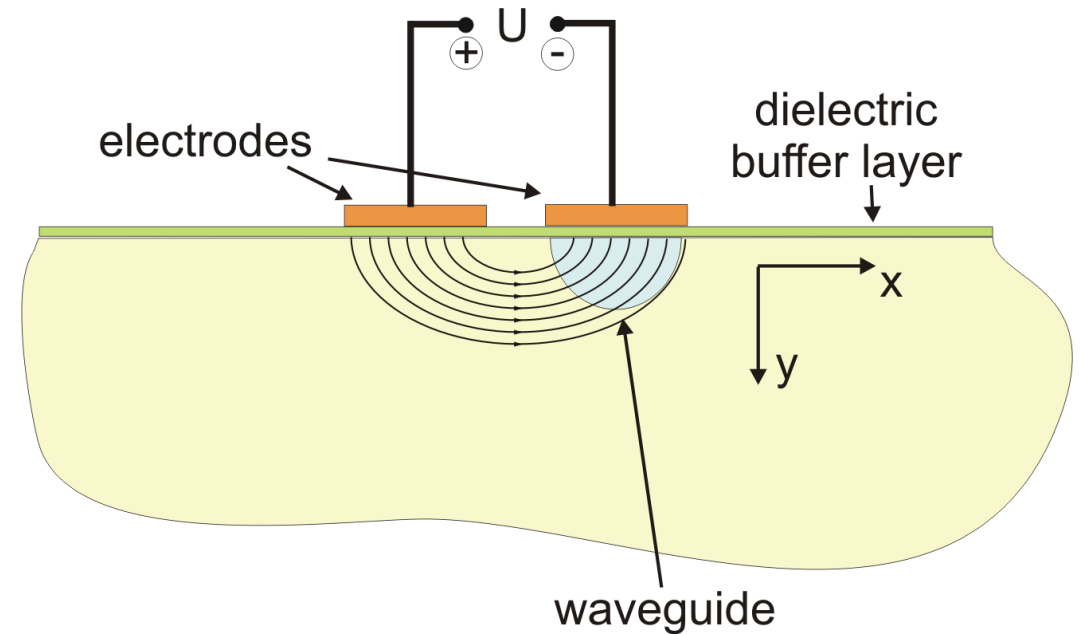
field component  
parallel to c - axis

- “Averaging” via integration over cross section:

$$\Delta n_{eff} = -\frac{n_e^3 r_{33}}{2} \frac{U}{G} \Gamma \quad \text{with} \quad \Gamma = \frac{G}{U} \frac{\iint E_{DC,y}(x, y) |E_{opt,y}(x, y)|^2 dx dy}{\iint |E_{opt,y}(x, y)|^2 dx dy}$$

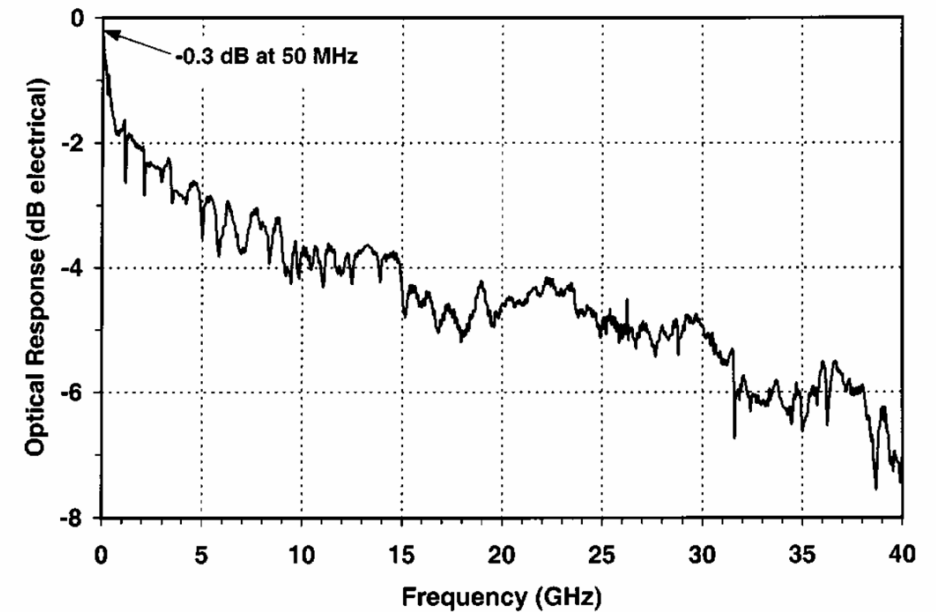
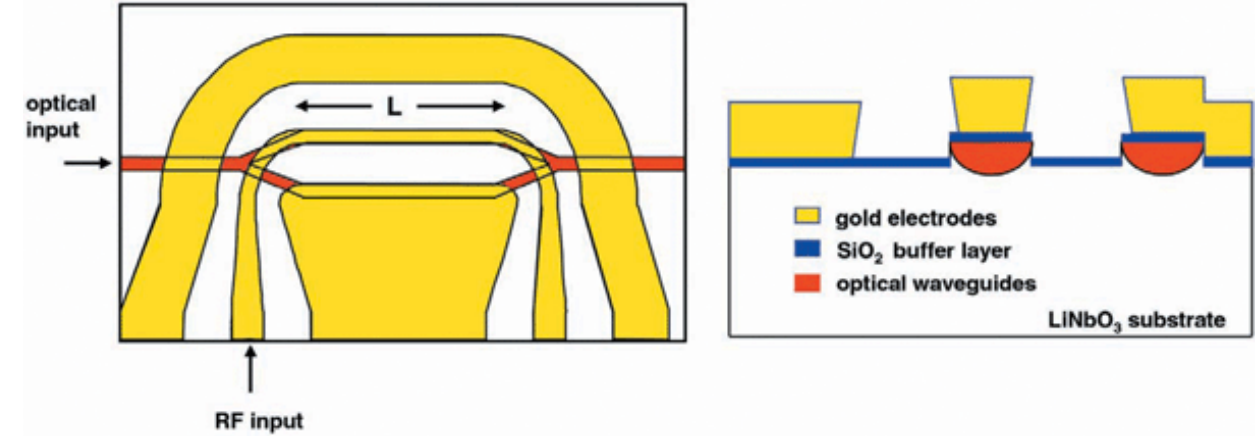
overlap integral

- Low driving voltages and high bandwidth

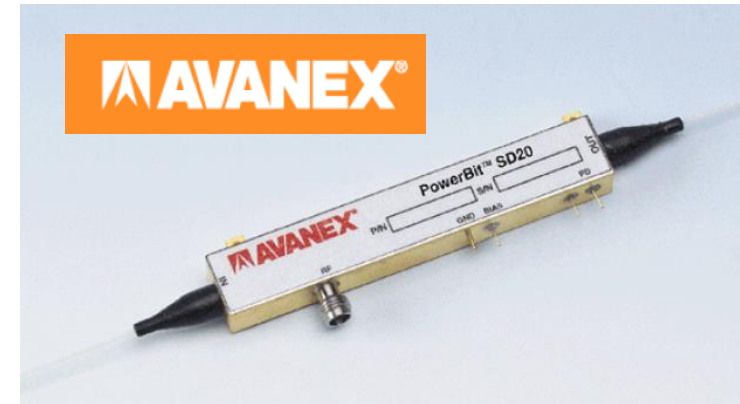


# Electro-optic modulation

- ▶ Mach-Zehnder modulator for high-data rate transmission systems [1]
- ▶ Sophisticated electrode design optimized for impedance and velocity matching
- ▶ RF-operation up to 40 GHz
- ▶ 5 V drive voltage (@ 40 GHz)

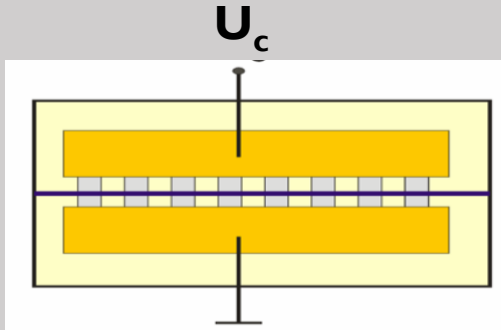


# Commercial products





# Polarization converter

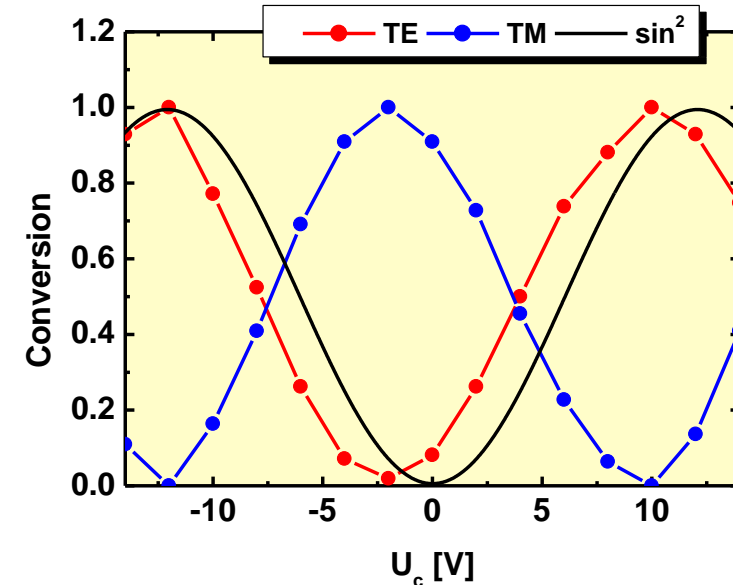
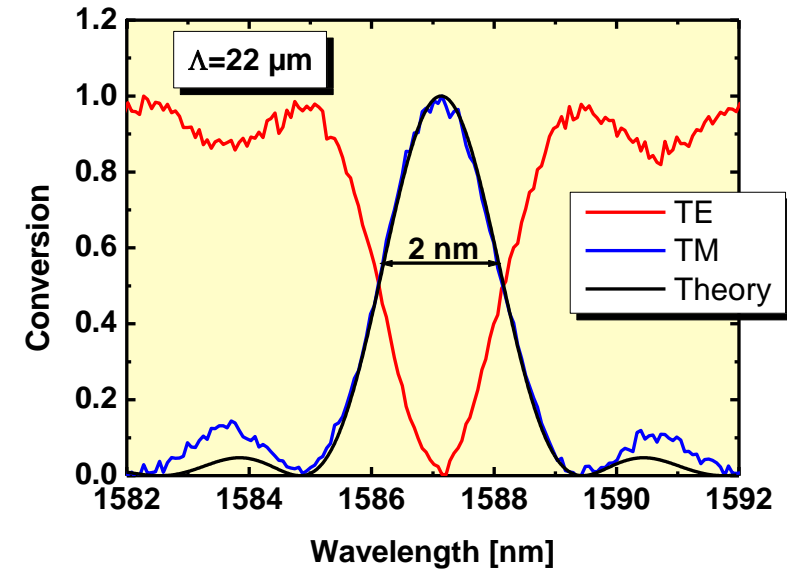


- ▶ Electro-optic wavelength selective polarisation conversion
- ▶ „Integrated optical Solc-Filter“
- ▶ Electro-optic coupling via non-diagonal coefficient  $r_{51}$  in a periodically poled waveguide

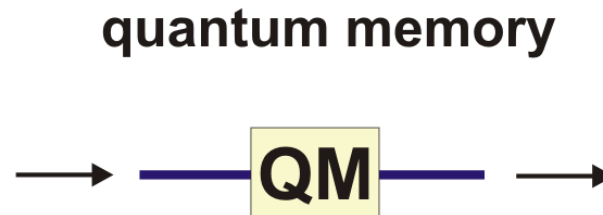
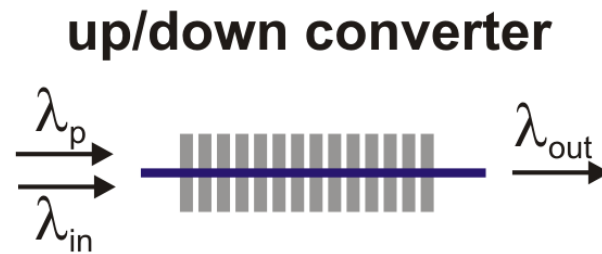
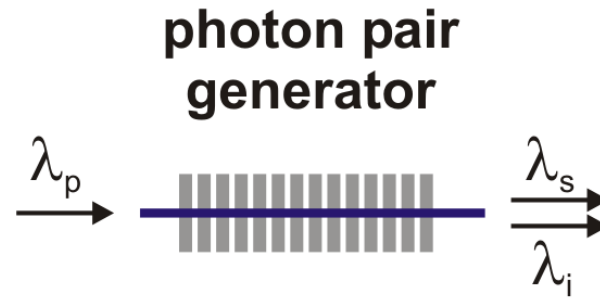
▶ **Poling period:**

$$\Lambda = \frac{\lambda}{n_{TM} - n_{TE}}$$

phase matching condition!

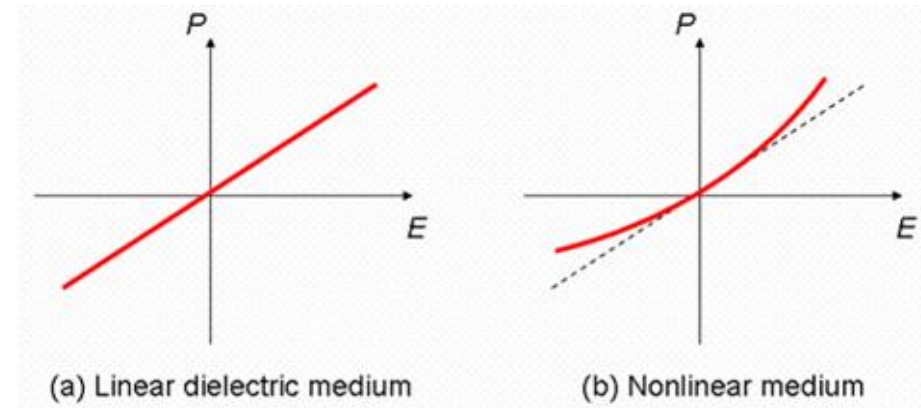


# Generation and storage



# Nonlinear optical polarization

- Nonlinearity in the dielectric polarization



$$\vec{P}(\vec{r}, t) = \epsilon_0 \chi(\vec{r}, t) \vec{E}(\vec{r}, t) \quad \vec{P}(\vec{r}, t) = \epsilon_0 \chi(\vec{r}, t, \vec{E}) \vec{E}(\vec{r}, t)$$

- Nonlinear polarization is the driving source for the generation of waves at new frequencies

non centrosymmetric crystal required

- Taylor expansion of nonlinear polarization

$$\vec{P} = \epsilon_0 (\chi^{(1)} \cdot \vec{E} + \chi^{(2)} : \vec{E} \vec{E} + \chi^{(3)} : \vec{E} \vec{E} \vec{E} + \dots)$$

nonlinear optics: optical & optical fields



# Selected second-order processes

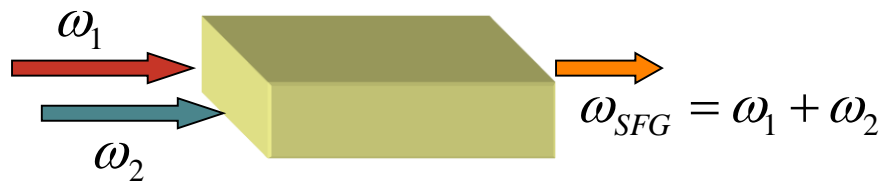
Second harmonic generation  
(SHG)



Parametric down-conversion  
(PDC)



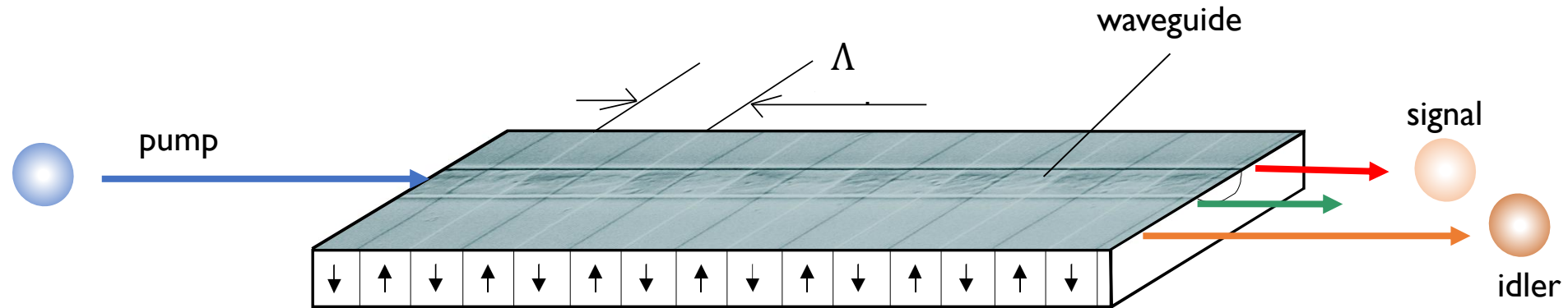
Sum frequency generation  
(SFG)



Difference frequency generation  
(DFG)



# A few words on parametric down-conversion



- ▶ energy and momentum conservation (quasi-phase-matching):

$$\omega_p = \omega_s + \omega_i$$

$$\beta_p = \beta_s + \beta_i + \frac{2\pi}{\Lambda}$$

- ▶ strong confinement of optical waves to small cross sections over long interaction length  $\Rightarrow$  high efficiency

$$\eta \propto d_{eff}^2 P_p L^2$$

- ▶ interaction length up to about **90 mm** can be possible

# First demonstrations of guided-wave PDC

Optical parametric fluorescence in Ti:LiNbO<sub>3</sub> channel waveguides

B. Hampel and W. Sohler

Universität-GH-Paderborn, Fachbereich Physik, Angewandte Physik  
Postfach 1621, D-4790 Paderborn, Fed. Rep. Germany

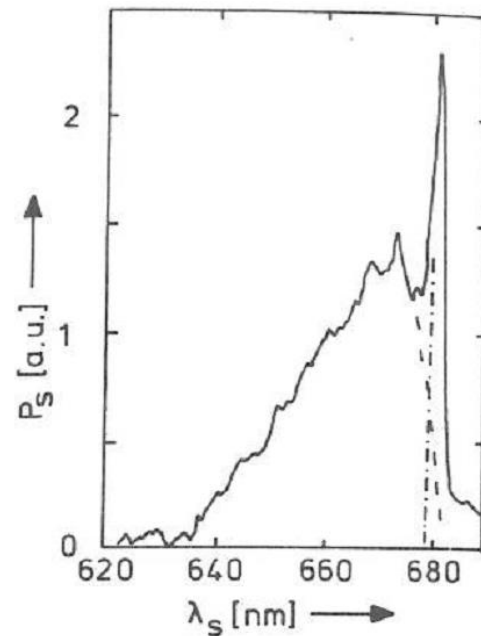


Figure: 4. Spatially filtered parametric fluorescence (signal part) from a 10 μm wide Ti:LiNbO<sub>3</sub> channel guide versus the wavelength; pump wavelength: 514 nm; waveguide temperature: 220°C.

## EFFICIENT QUASIPHASE-MATCHED GENERATION OF PARAMETRIC FLUORESCENCE IN ROOM TEMPERATURE LITHIUM NIOBATE WAVEGUIDES

P. Baldi, S. Nouh, M. de Micheli, D. B. Ostrowsky, D. Delacourt, X. Banti and M. Papuchon

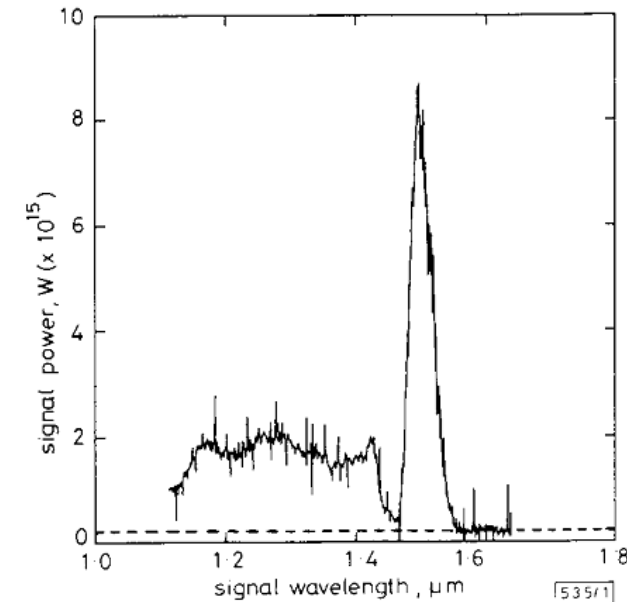


Fig. 1 Trace of parametric fluorescence for 7 μm wide guide, 20 μm domain inversion period, 0.811 μm pump wavelength and 10 ± 2 mW guided pump power

Peak parametric fluorescence power at 1.5 μm is  $8 \times 10^{-15}$  W  
----- 'signal' observed when using an identical guide and pump power in a region without domain inversion

- [1] B. Hampel, W. Sohler, SPIE Proc. 651 „Integrated Optical Circuit Engineering III“, pp. 229-234 (1986)
- [2] P. Baldi et al., Electron. Lett. 29, 1539 (1993)



# Frequency converters

## Stationary qubit-systems

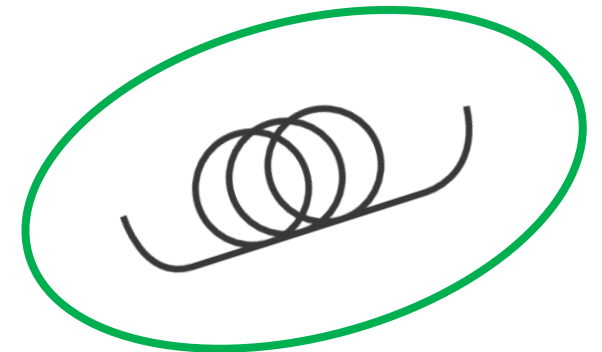
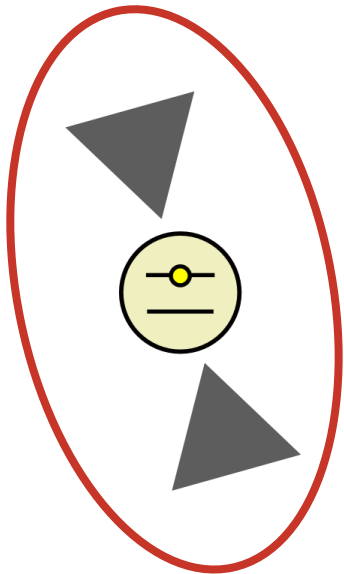
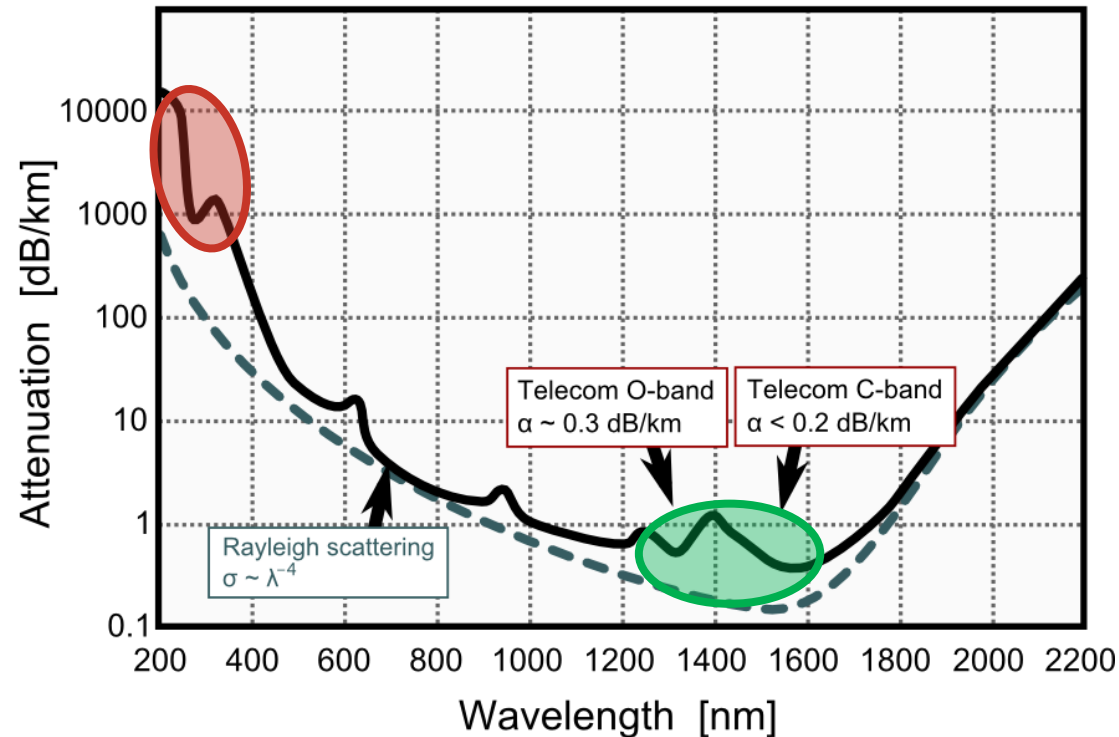
e.g. cold atoms/ions,  
solid state systems  
UV-/Visible/NIR

Bridging the gap by  
**frequency conversion**

## Photonic state transfer

requires  
telecommunication  
wavelengths (IR)

Attenuation in silica fibers



# Recent examples from the literature

PRL **109**, 147404 (2012) PHYSICAL REVIEW LETTERS week ending 5 OCTOBER 2012

**Visible-to-Telecom Quantum Frequency Conversion of Light from a Single Quantum Emitter**

Sebastian Zaske,<sup>1</sup> Andreas Lenhard,<sup>1</sup> Christian A. Keßler,<sup>2</sup> Jan Kettler,<sup>2</sup> Christian Hepp,<sup>1</sup> Carsten Arend,<sup>1</sup> Roland Albrecht,<sup>1</sup> Wolfgang-Michael Schulz,<sup>2</sup> Michael Jetter,<sup>2</sup> Peter Michler,<sup>2</sup> and Christoph Becher<sup>1,\*</sup>

<sup>1</sup>Fachrichtung 7.2 (Experimentalphysik), Universität des Saarlandes, Campus E2.6, 66123 Saarbrücken, Germany  
<sup>2</sup>Institut für Halbleitertechnik und Funktionelle Grenzflächen and Research Center SCoPE, Universität Stuttgart, 70569 Stuttgart, Germany  
 (Received 18 June 2012; published 4 October 2012)

[1]

Phys. Rev. Lett. **109**, 147404 (2012)

ARTICLES PUBLISHED ONLINE 3 OCTOBER 2010 | DOI: 10.1038/NPHOTON.2010.221 nature photonics

**Quantum transduction of telecommunications-band single photons from a quantum dot by frequency upconversion**

Matthew T. Rakher<sup>1</sup>, Lijun Ma<sup>2</sup>, Oliver Slattery<sup>2</sup>, Xiao Tang<sup>2\*</sup> and Kartik Srinivasan<sup>1\*</sup>

[2]

Nature Photon **4**, 786 (2010)

**Frequency down-conversion of 637 nm light to the telecommunication band for non-classical light emitted from NV centers in diamond**

[3]

Rikizo Ikuta,<sup>1,\*</sup> Toshiaki Kobayashi,<sup>1</sup> Shuto Yasui,<sup>1</sup> Shigehito Miki,<sup>2</sup> Taro Yamashita,<sup>2</sup> Hirotaka Terai,<sup>2</sup> Mikio Fujiwara,<sup>3</sup> Takashi Yamamoto,<sup>1</sup> Masato Koashi,<sup>3</sup> Masahide Sasaki,<sup>4</sup> Zhen Wang,<sup>2,5</sup> and Nobuyuki Imoto<sup>1</sup>

<sup>1</sup>Graduate School of Engineering Science, Osaka University, Toyonaka, Osaka 560-8531, Japan

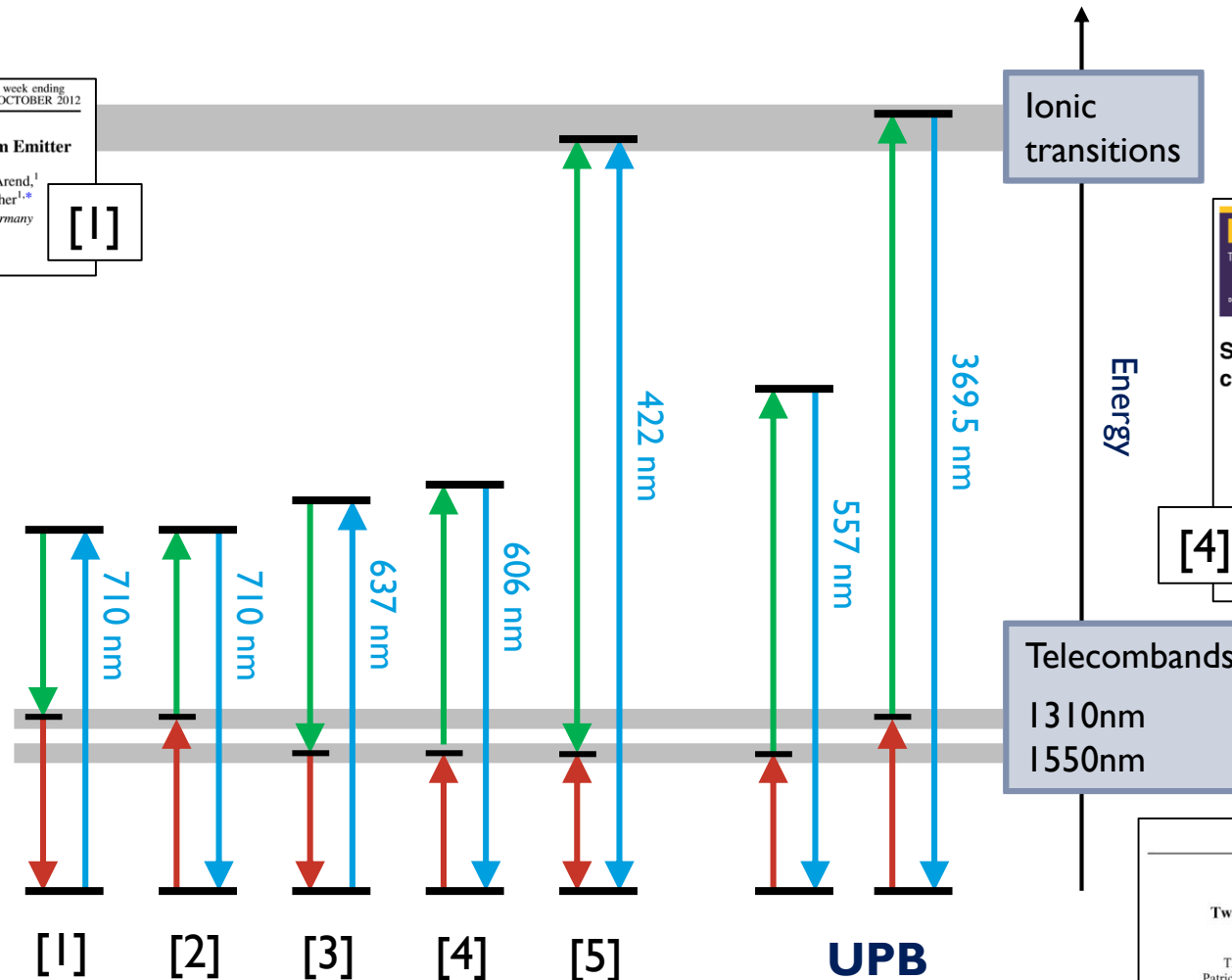
<sup>2</sup>Advanced ICT Research Institute, National Institute of Information and Communications Technology (NICT), Kobe 651-2492, Japan

<sup>3</sup>Photon Science Center, The University of Tokyo, Bunkyo-ku, Tokyo 113-8656, Japan

<sup>4</sup>Advanced ICT Research Institute, National Institute of Information and Communications Technology (NICT), Koganei, Tokyo 184-8795, Japan

<sup>5</sup>Shanghai Center for Superconductivity, Shanghai Institute of Microsystem and Information Technology, Chinese Academy of Sciences, R3317, 865 Changning Road, Shanghai 200050, China

Opt. Exp. **22**, 11205 (2014)



Recent quantum frequency converters

**New Journal of Physics**  
 The open access journal at the forefront of physics  
 Deutsche Physikalische Gesellschaft DPG | IOP Institute of Physics

**Storage of up-converted telecom photons in a doped crystal**

Nicolas Maring<sup>1</sup>, Kutlu Kutluer<sup>1</sup>, Joachim Cohen<sup>1,3</sup>, Matteo Cristiani<sup>1</sup>, Margherita Mazzera<sup>1</sup>, Patrick M Ledingham<sup>1</sup> and Hugues de Riedmatten<sup>1,2</sup>

<sup>1</sup>ICFO-Institut de Ciències Fotòniques, Mediterranean Technology Park, E-08860 Castelldefels (Barcelona), Spain  
<sup>2</sup>ICREA-Institució Catalana de Recerca i Estudis Avançats, E-08015 Barcelona, Spain  
 E-mail: patrick.ledingham@icfo.es

Received 11 July 2014, revised 12 September 2014  
 Accepted for publication 1 October 2014  
 Published 11 November 2014  
 New Journal of Physics **16** (2014) 113021  
 doi:10.1088/1367-2630/16/11/113021

New J. Phys. **16**, 113021 (2014)

PHYSICAL REVIEW APPLIED **10**, 044012 (2018)

**Two-Way Photonic Interface for Linking the Sr<sup>+</sup> Transition at 422 nm to the Telecommunication C Band**

Thomas A. Wright,<sup>1,\*</sup> Robert J. A. Francis-Jones,<sup>1,2</sup> Corin B. E. Gawith,<sup>3</sup> Jonas N. Becker,<sup>2</sup> Patrick M. Ledingham,<sup>2</sup> Peter G. R. Smith,<sup>3</sup> Joshua Nunn,<sup>2</sup> Peter J. Mosley,<sup>1</sup> Benjamin Brecht,<sup>2</sup> and Ian A. Walmsley<sup>2</sup>

<sup>1</sup>Centre for Photonics and Photonic Materials, Department of Physics, University of Bath, Bath BA2 7AY, United Kingdom  
<sup>2</sup>Clarendon Laboratory, University of Oxford, Parks Road, Oxford OX1 3PU, United Kingdom  
<sup>3</sup>Optoelectronics Research Centre, University of Southampton, Southampton SO17 1BJ, United Kingdom

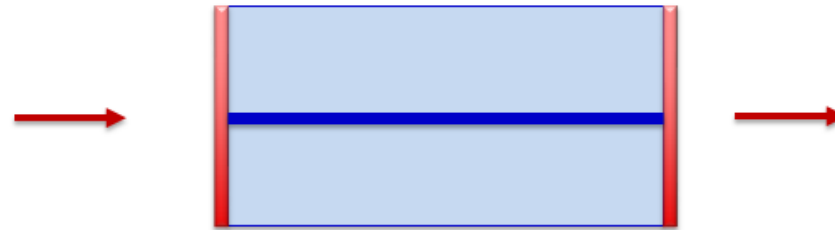
[5]

Phys. Rev. Applied **10**, 044012 (2018)

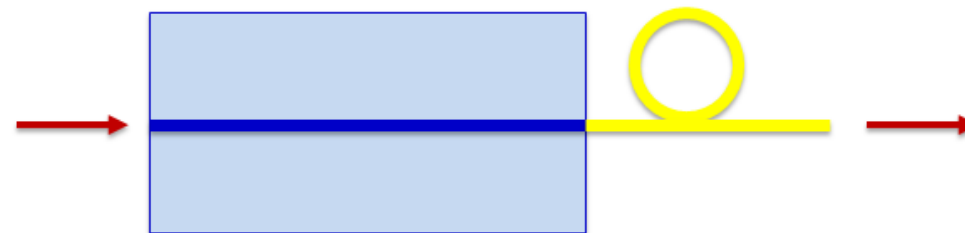


# Interfacing

dielectric mirror coating



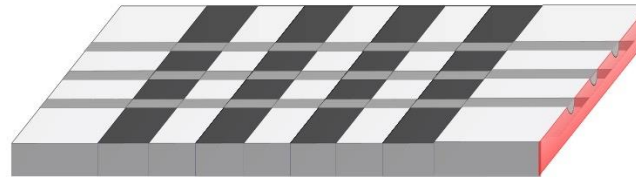
fiber waveguide coupling



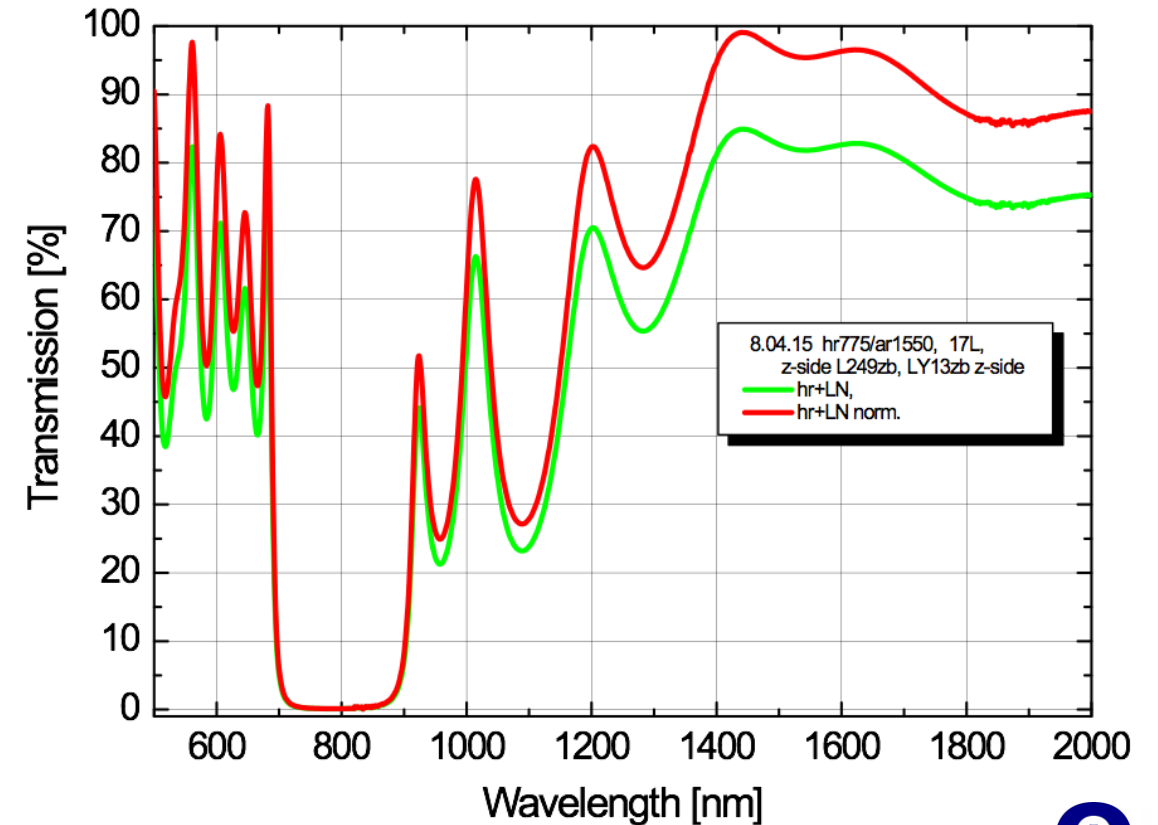
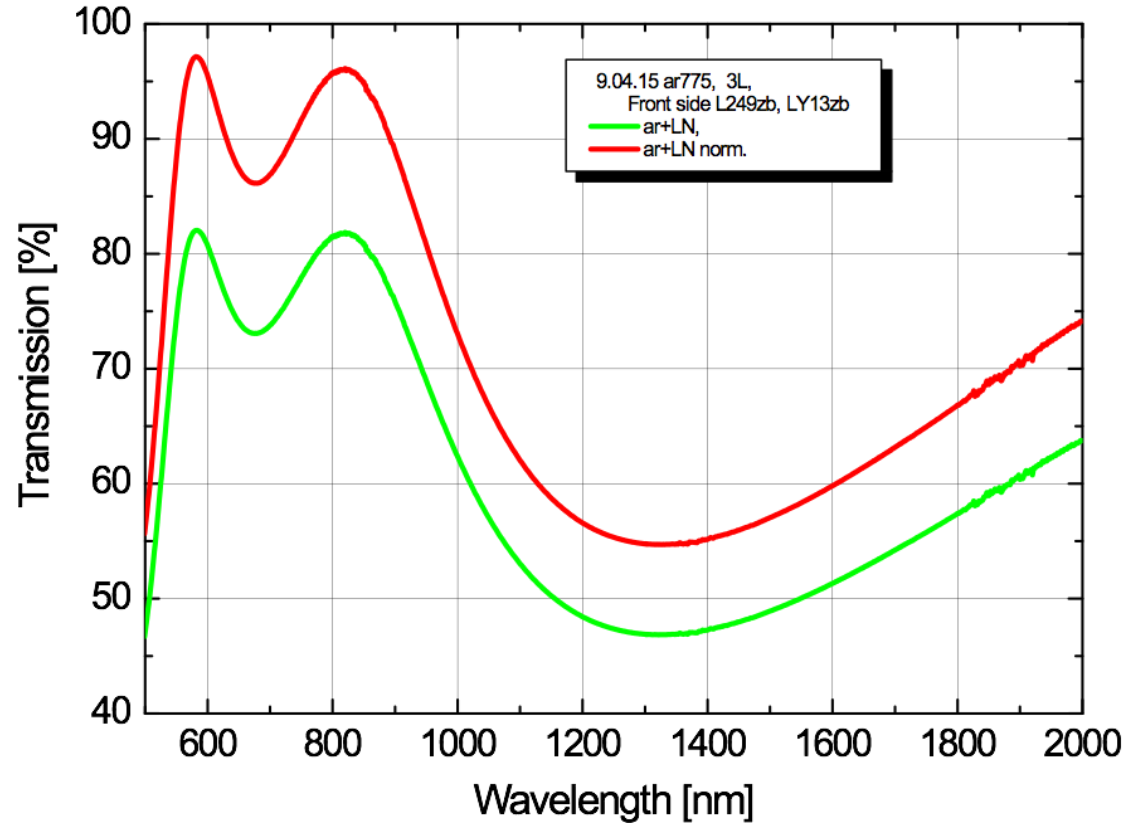


# Dielectric endfacet coatings

Ti:PPLN  
waveguide

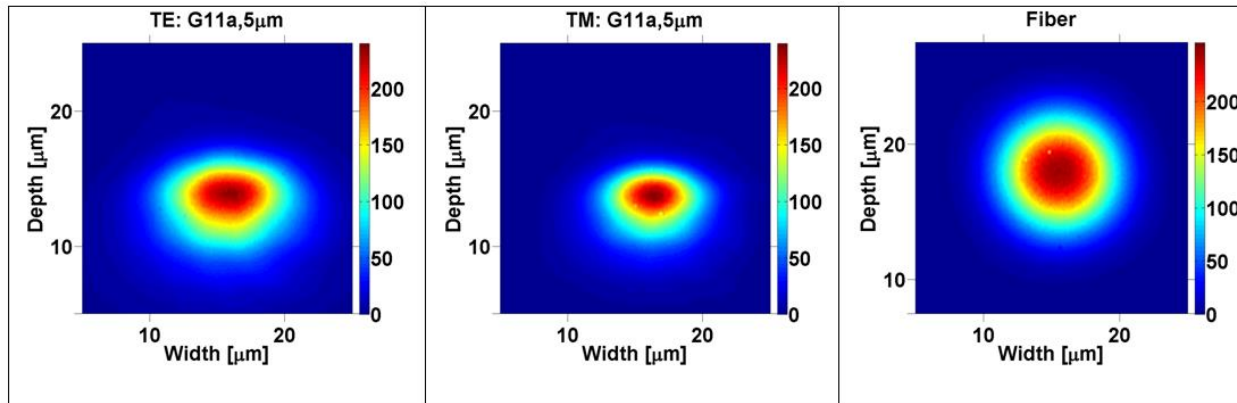


Coatings

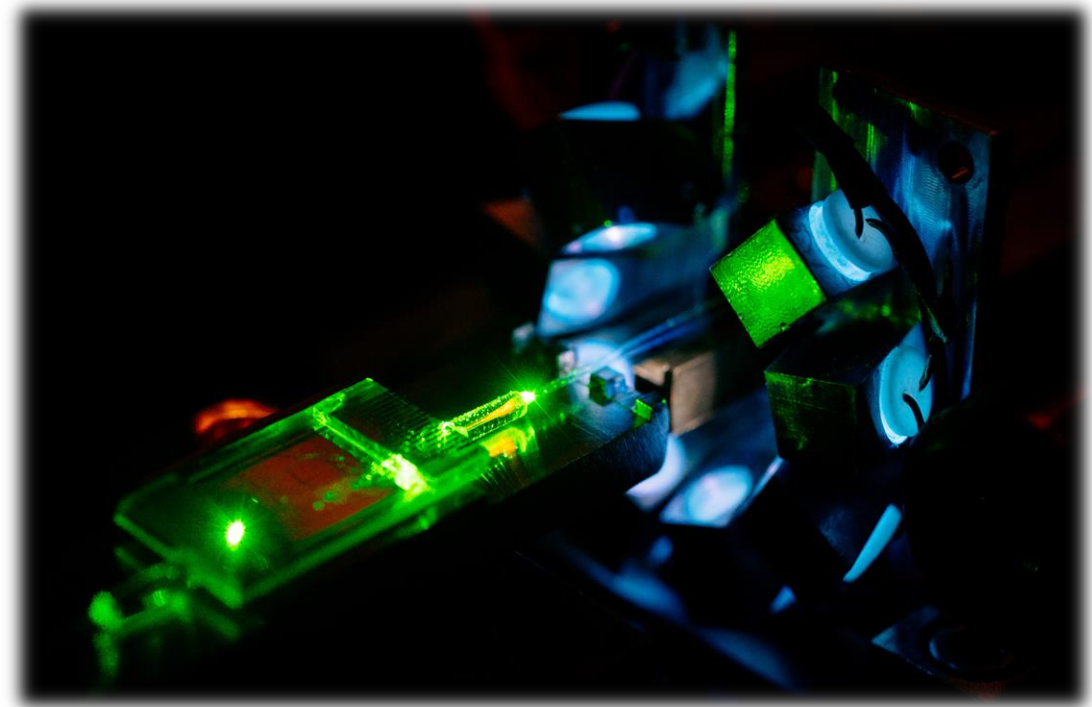


# Pigtailing (waveguide-fibre coupling)

- ▶ Coupling between waveguide modes and single-mode fibers
- ▶ Good mode overlap of waveguide modes with standard single mode fibers:



- ▶ Coupling loss  $< 1$  dB possible without any specific tailoring of waveguide modes
- ▶ Optimization of waveguide fabrication parameter can further minimize coupling losses



© Paderborn University: Besim Mazhiqi

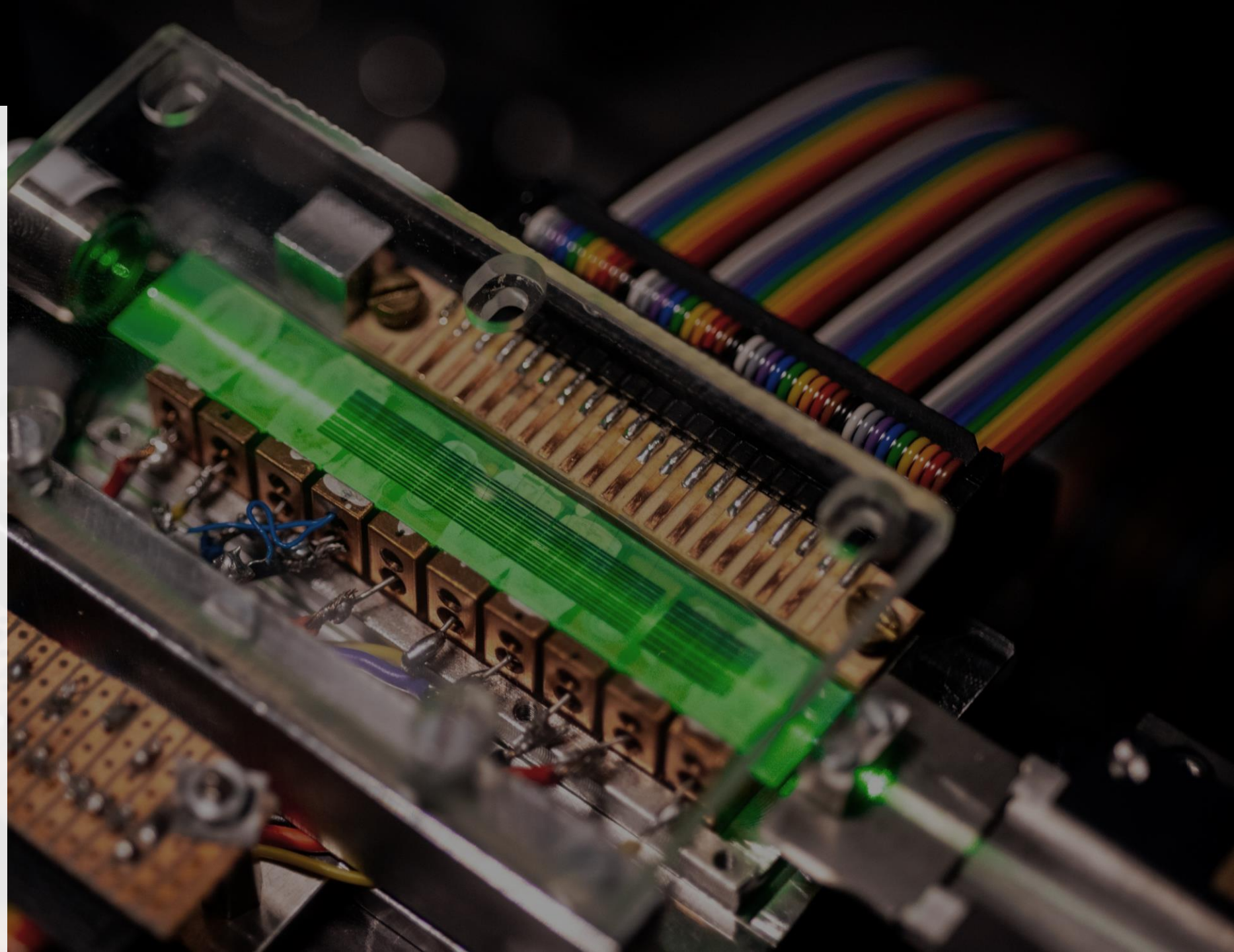
# Outline

Underlying  
concepts

Device  
toolbox

**Fabrication  
technology**

HOM-on-chip  
circuit

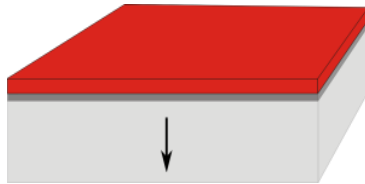


# Waveguide fabrication

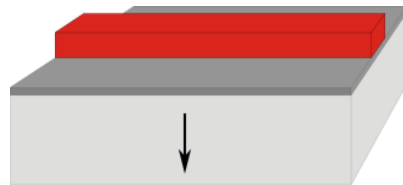


# Waveguide fabrication

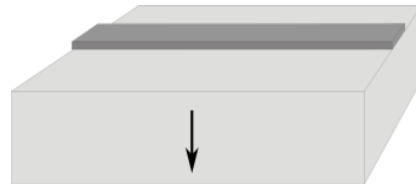
## Titanium-indiffused waveguide fabrication



Titanium deposition and photoresist spin coating

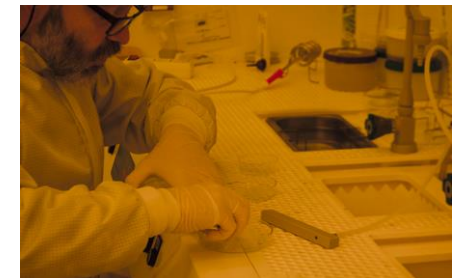
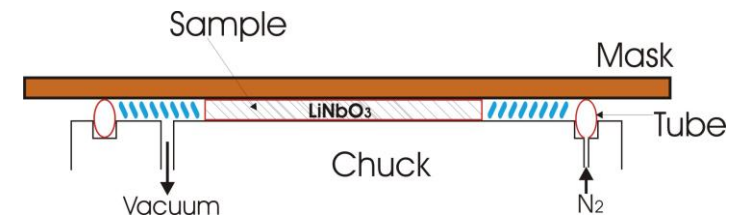
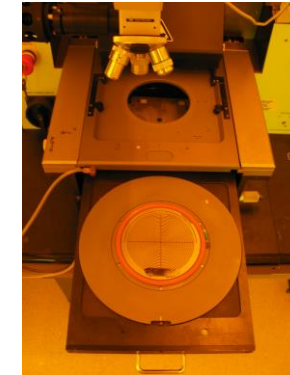
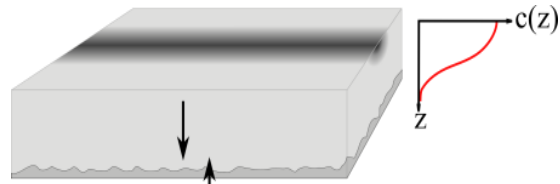


Photolithographic patterning



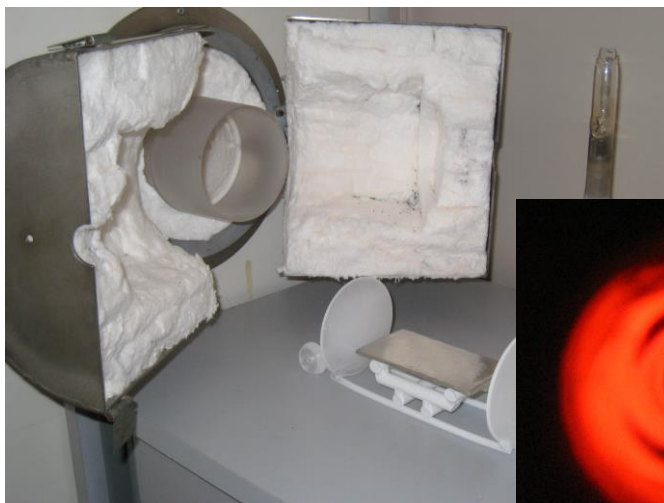
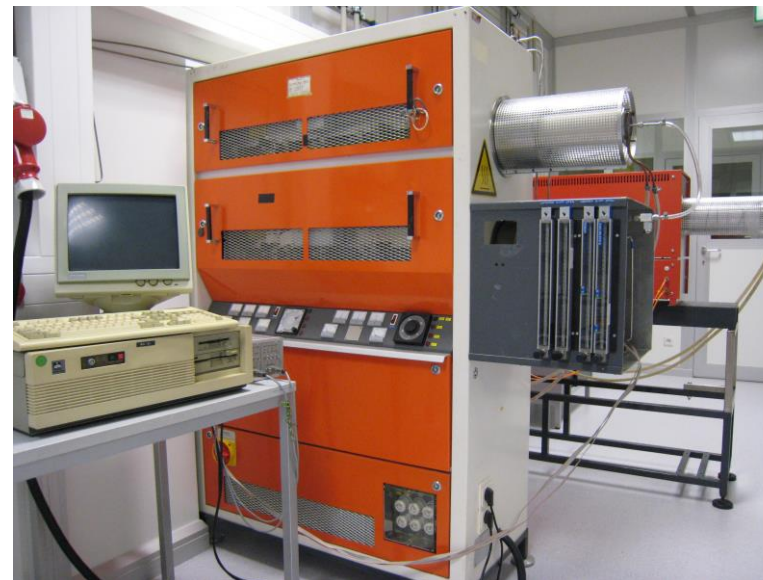
Ti-etching and photoresist removal

Ti-indiffusion



# Waveguide indiffusion

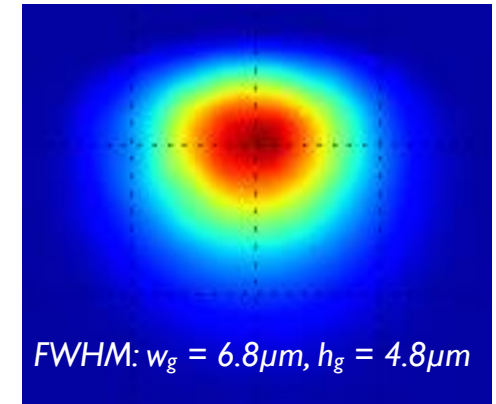
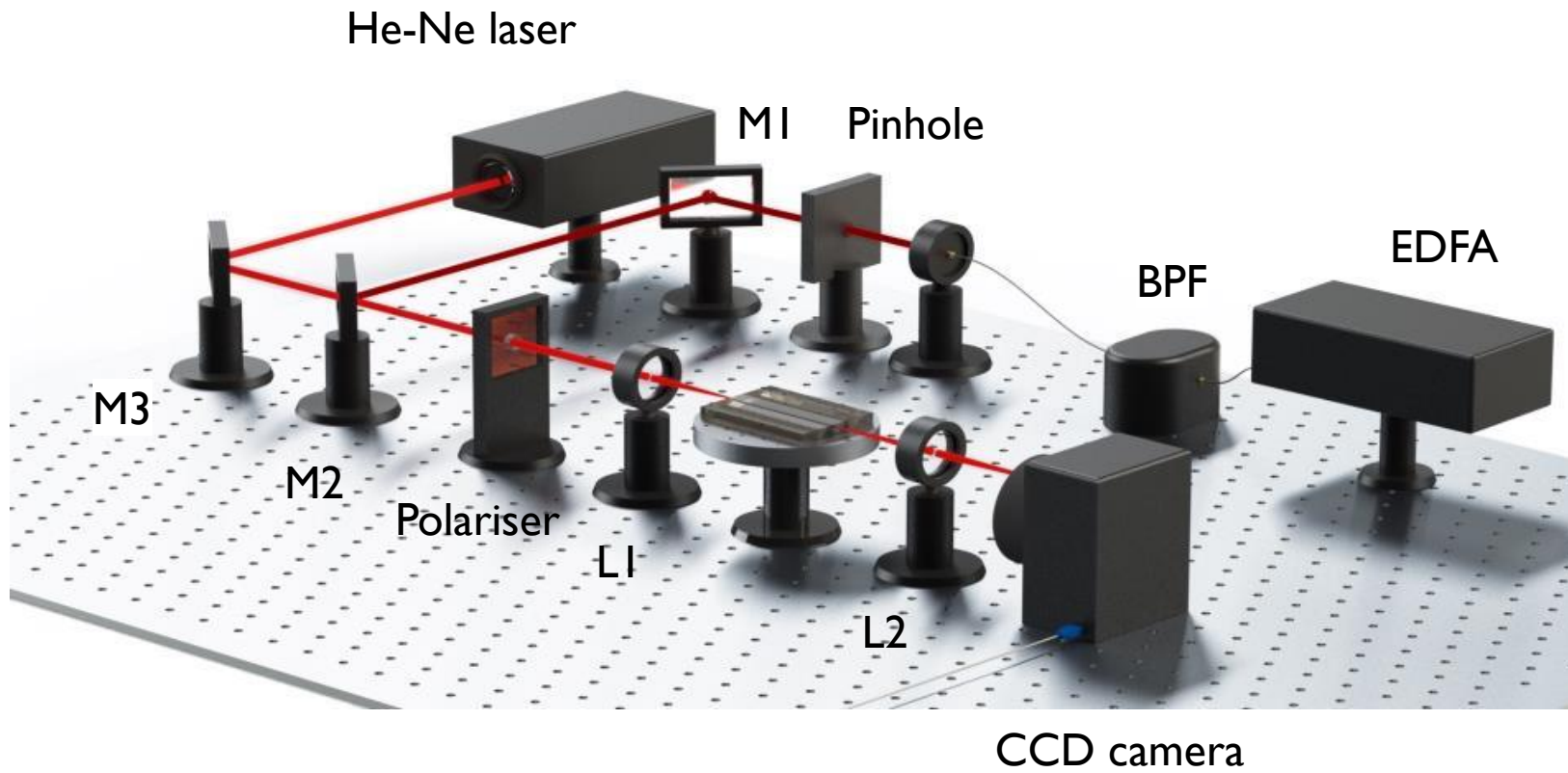
- ▶ Diffusion furnace: Centrotherm
- ▶ Waveguide NIR  
1060°C for 8h in O<sub>2</sub>
- ▶ Waveguide MIR  
1060°C for 31h in O<sub>2</sub> and Ar



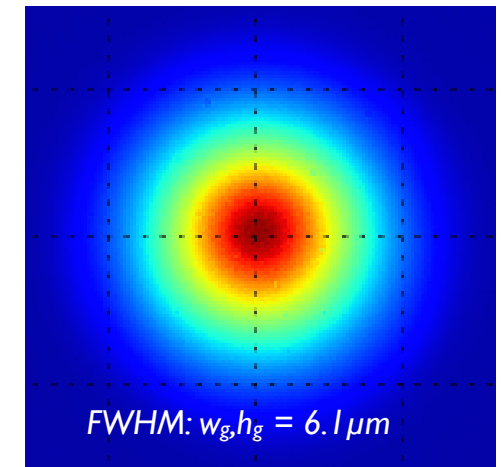
## Diffusion in Pt-Box

avoid of out-diffusion  
protection against particles

# Mode size measurements

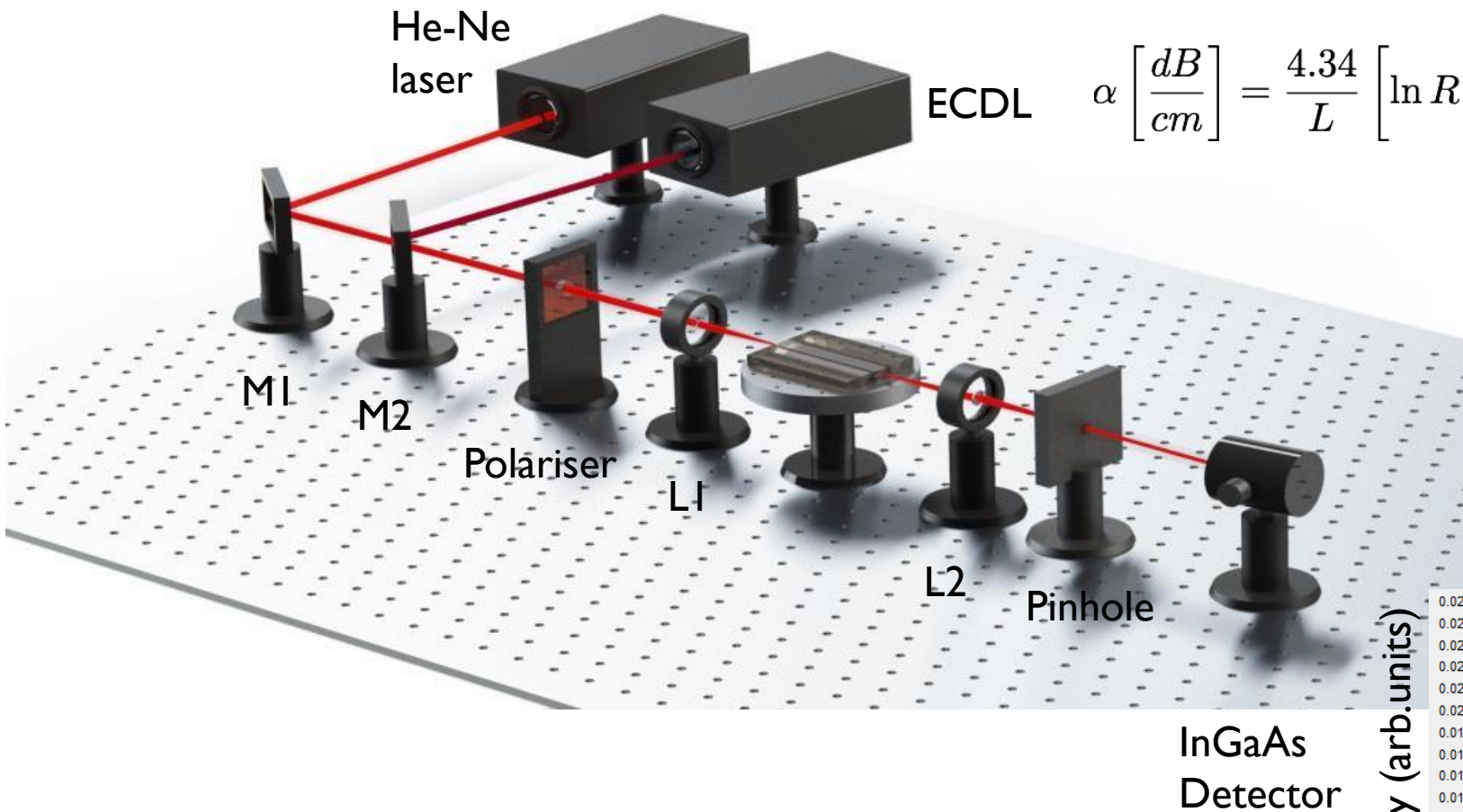


$Mode_{guide}$

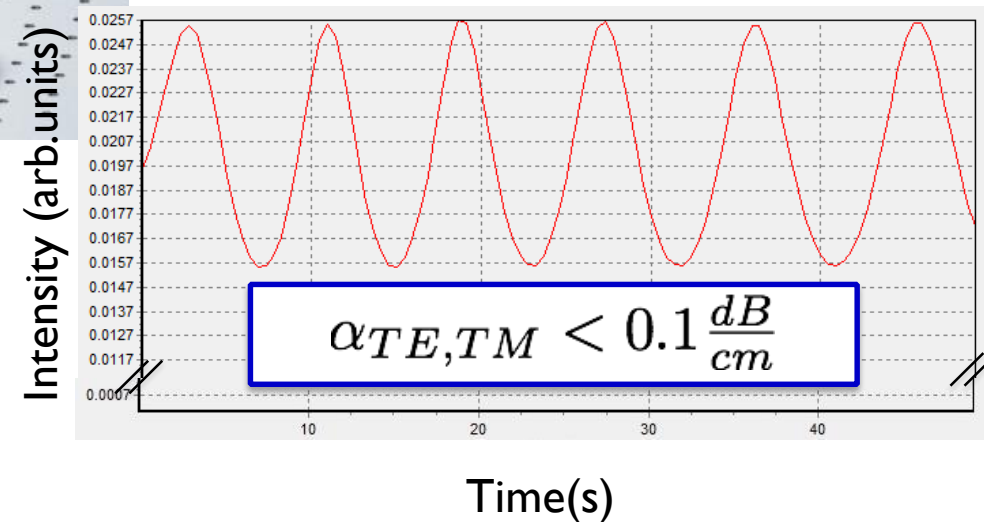


$Mode_{fiber}$

# Fabry-Perot loss measurement



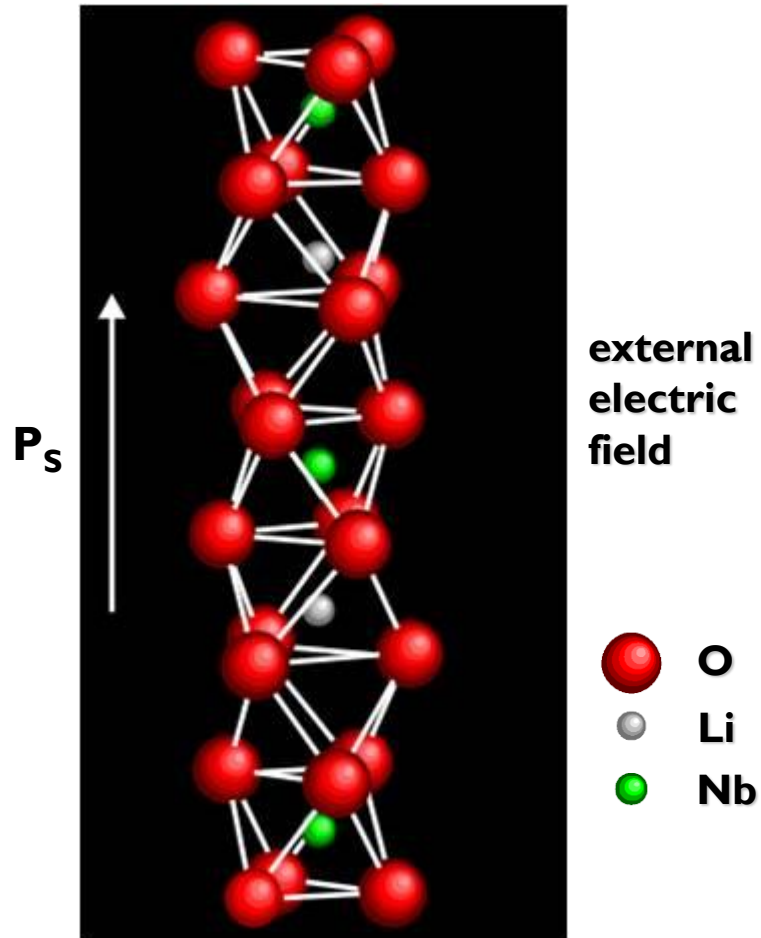
$$\alpha \left[ \frac{dB}{cm} \right] = \frac{4.34}{L} \left[ \ln R + \ln 2 - \ln \left( \frac{T_{max} - T_{min}}{T_{max} + T_{min}} \right) \right]$$





# Periodic poling

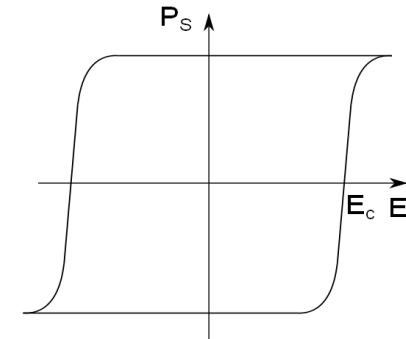
# Periodic poling of lithium niobate



(compare V. Gopalan et al.)

## Ferroelectric Phase:

- stacking of  $\text{Li}^+$  and  $\text{Nb}^{5+}$  relative to  $\text{O}^{2-}$  leads to spontaneous polarization ( $P_s$ )



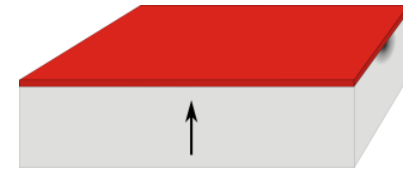
- $E_c = 21 \text{ kV/mm}$
- periodic  $P_s$ -inversion → domain grating
- domain grating →  $\chi^{(2)}$ -grating

# Periodic poling of lithium niobate

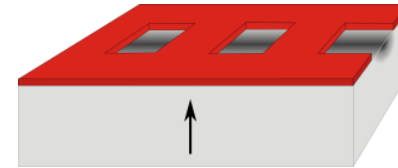


## Periodic domain inversion

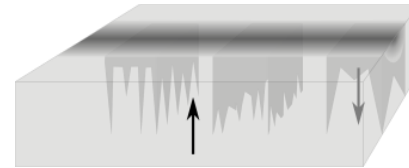
Photoresist coating



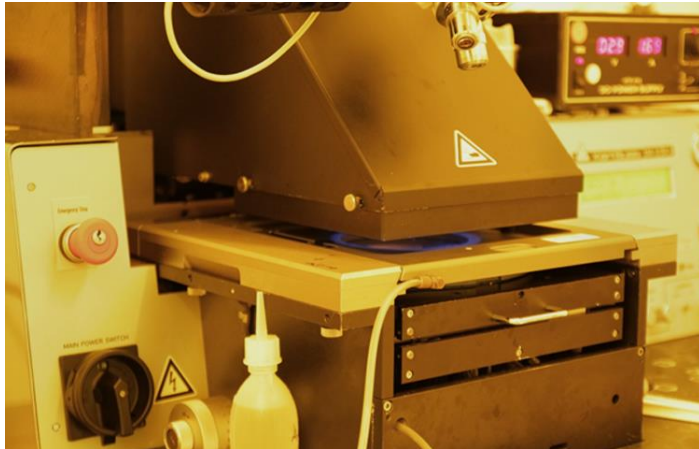
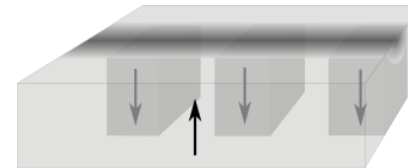
Photolithographic patterning



Domain growth under pulsed HV application

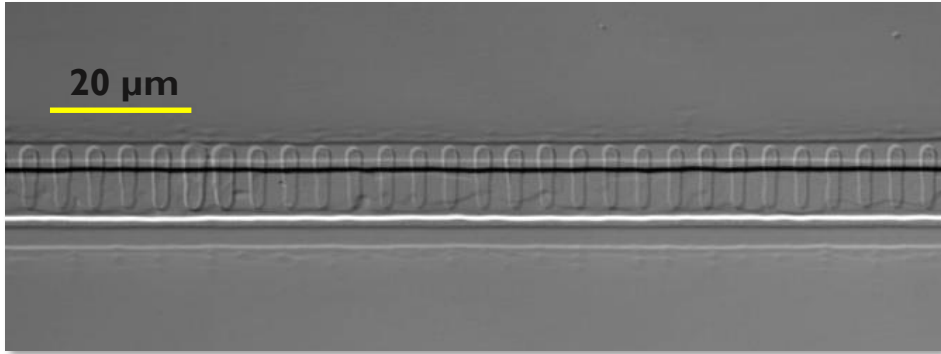


Periodically inverted domains



# Example waveguide

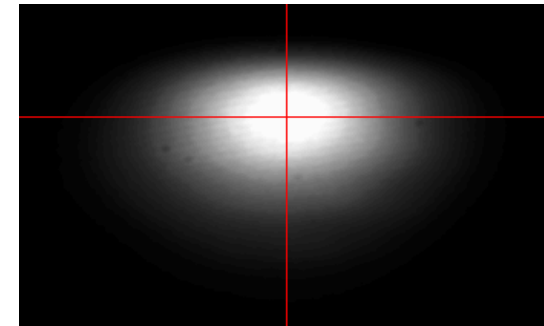
## Lithium niobate waveguide with 4.5 $\mu\text{m}$ poling



- ▶ Both polarizations guided
- ▶ Low propagation losses:  
 $\sim 0.02 \text{ dB/cm}$
- ▶ Coupling to single-mode fibre:  
 $\text{efficiency} > 85\%$
- ▶ Linear and nonlinear characterization  
(losses, modes, SHG/SFG/PDC)

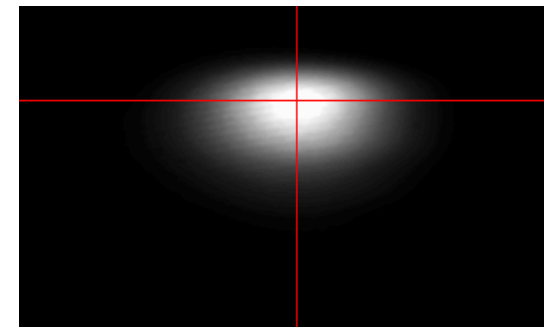
Mode profiles @ 1550nm  
(z-cut  $\text{Ti:LiNbO}_3$ )

TE-mode



$6.0 \times 4.2 \mu\text{m}^2$

TM-mode



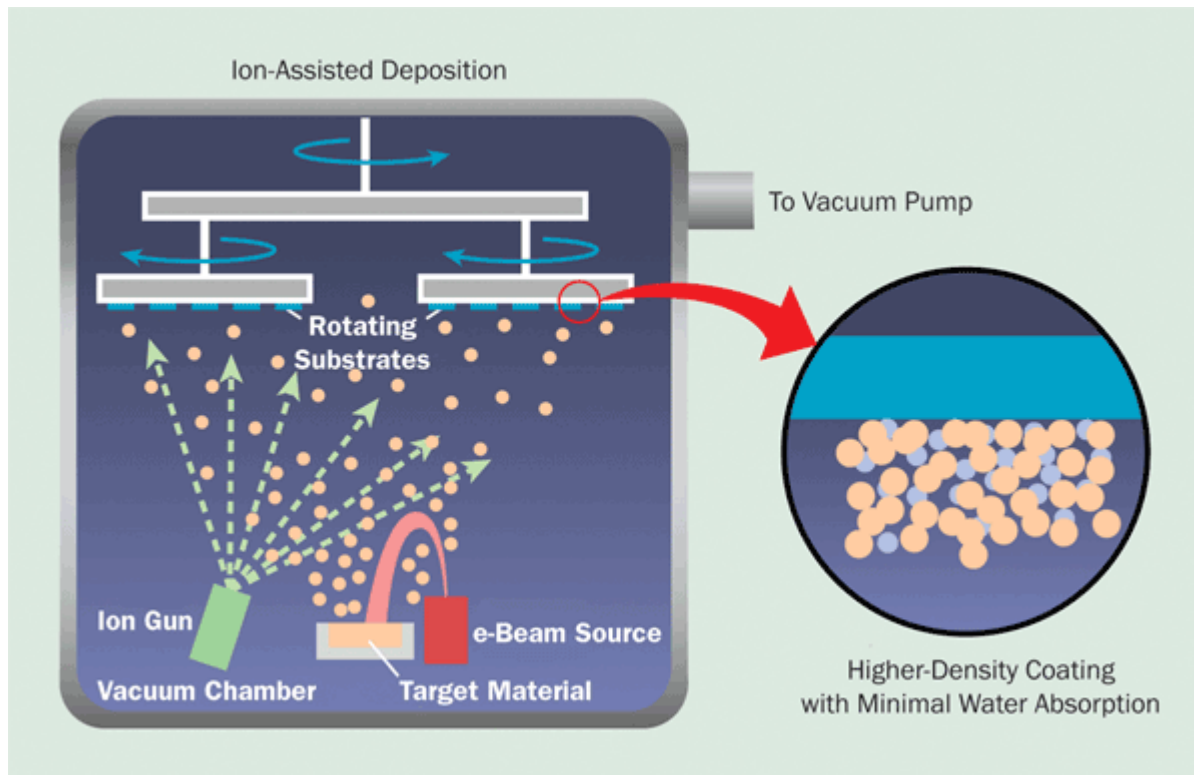
$4.3 \times 2.9 \mu\text{m}^2$



# Dielectric coatings

# Dielectric coating technique

## Ion Assisted Deposition (IAD)

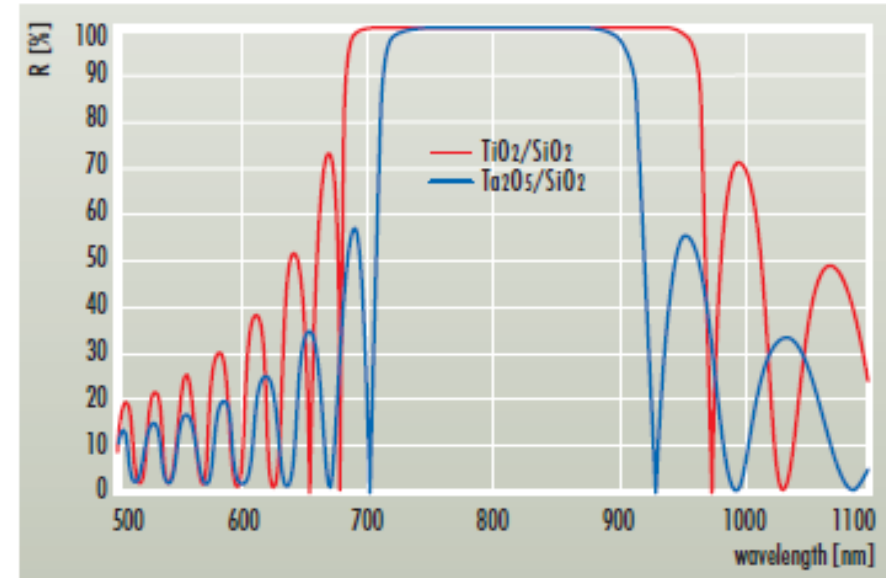


# Mirrors and partial reflectors

## Quarter wave stack

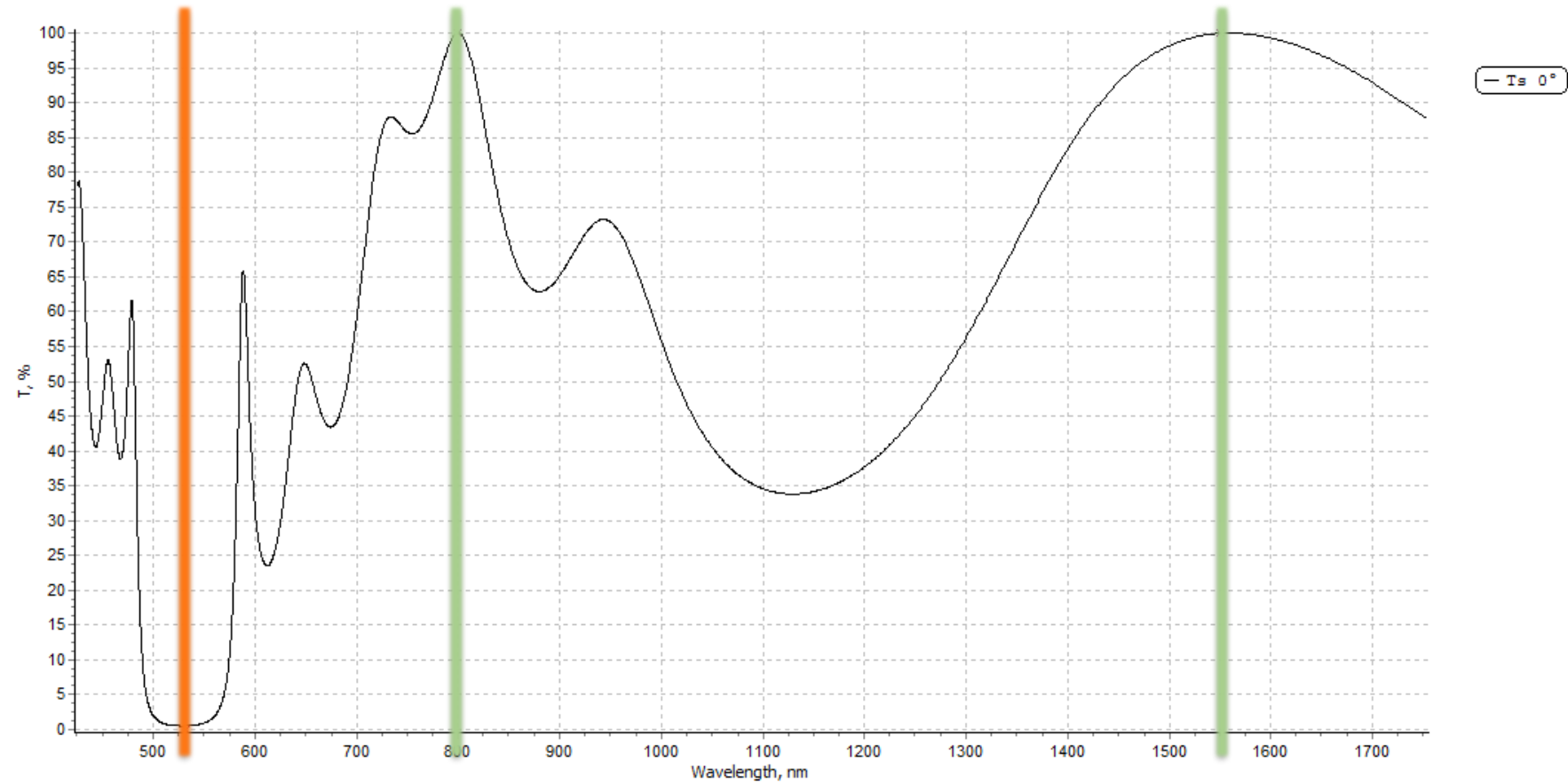


A quarter wave stack consisting of layers with equal optical thickness



Reflectivity spectra of quarter wave stacks consisting of 15 pairs of  $\text{Ta}_2\text{O}_5/\text{SiO}_2$  and  $\text{TiO}_2/\text{SiO}_2$

# AR/HR coatings



N = 12

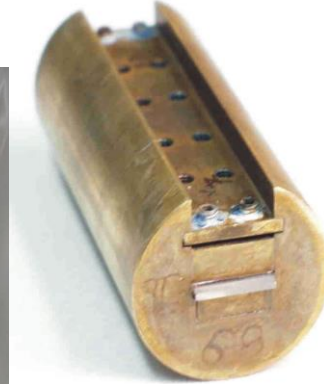
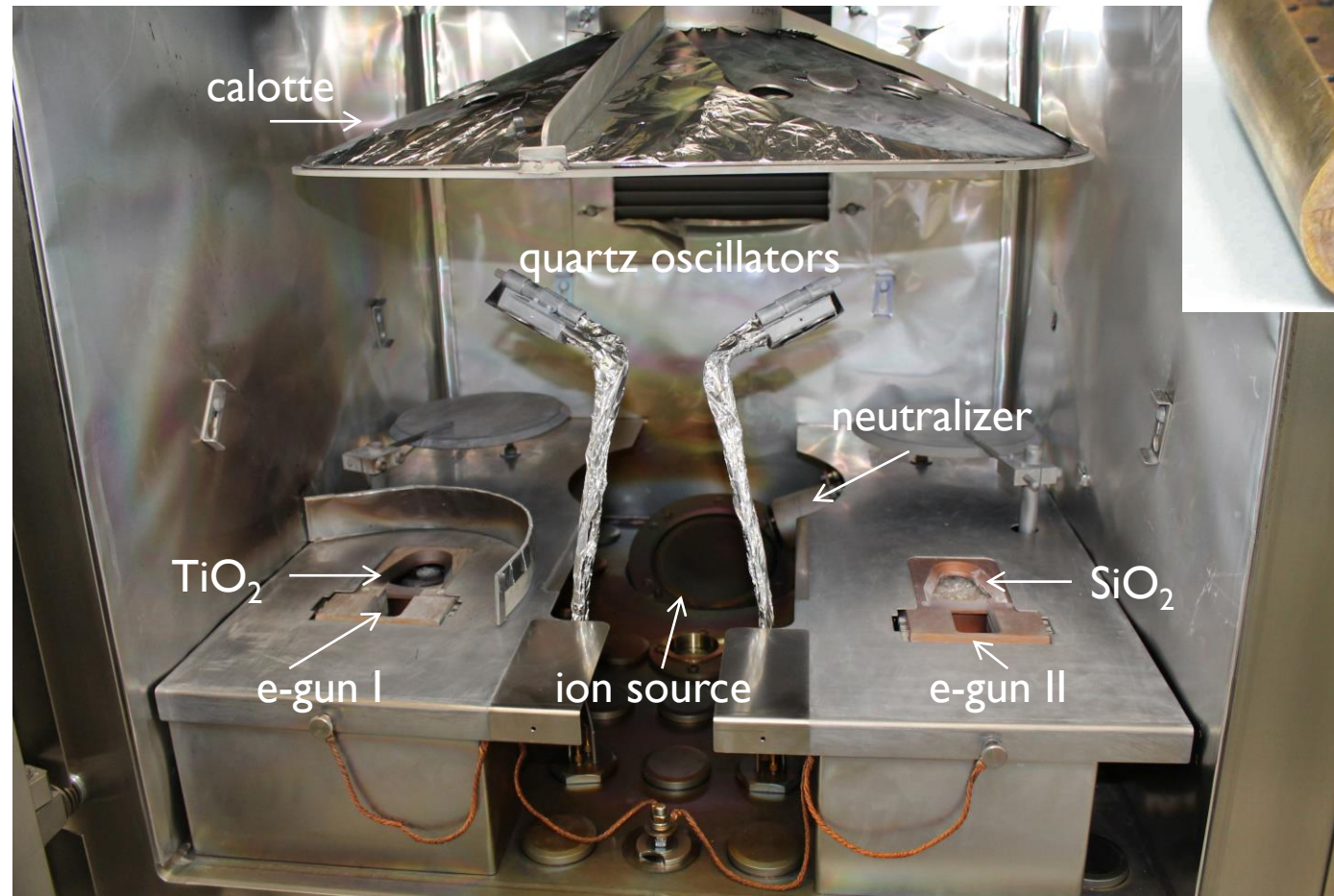
Th = 1489.3



# Our coating machine

View inside the coating machine

Sample holder



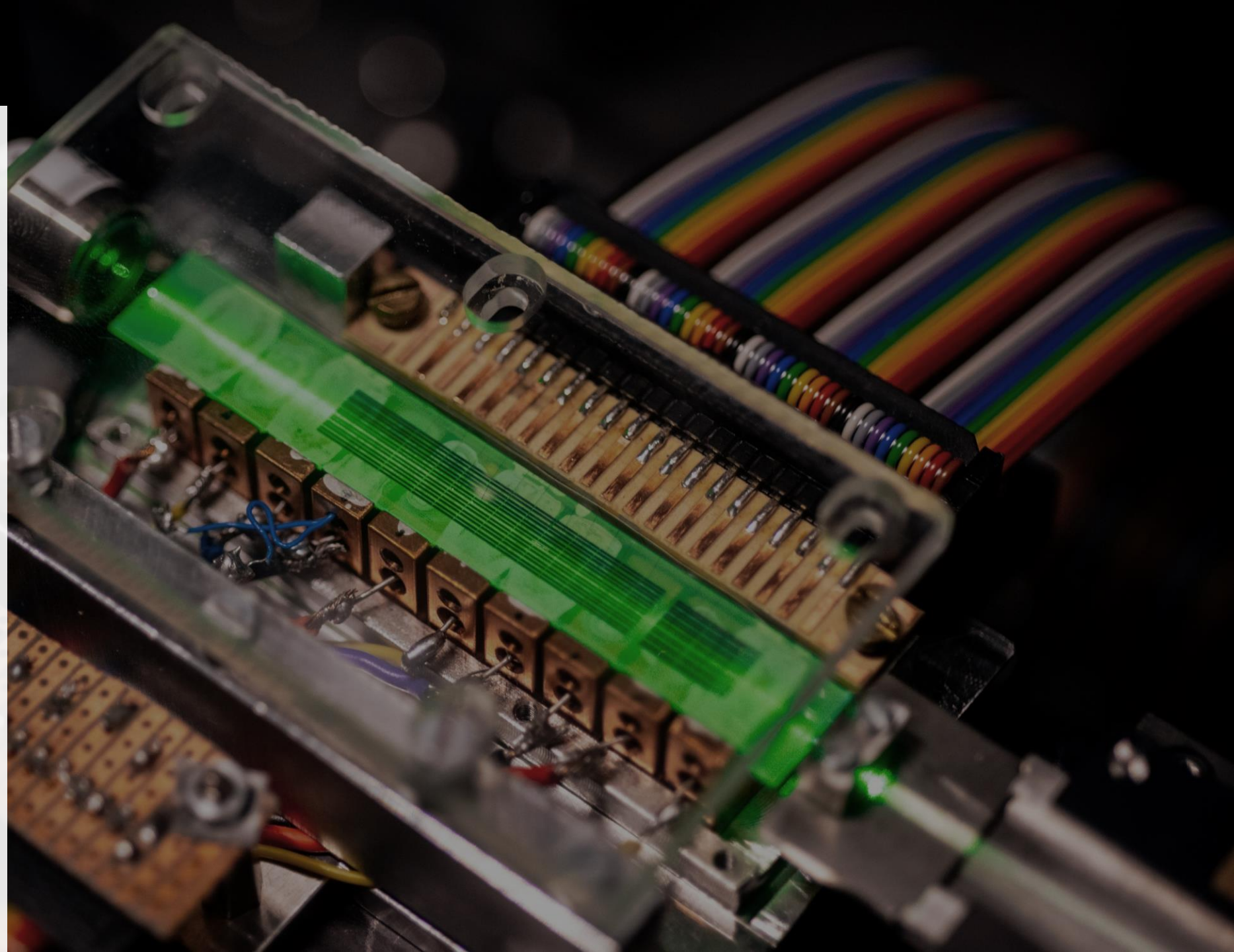
# Outline

Underlying  
concepts

Device  
toolbox

Fabrication  
technology

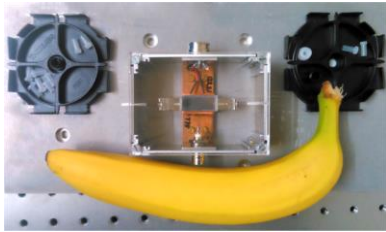
**HOM-on-chip  
circuit**





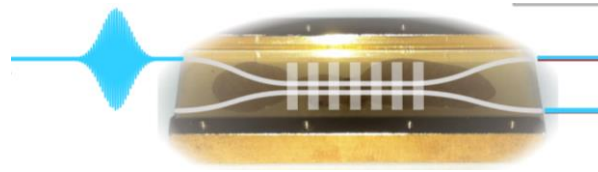
# Some quantum devices

## Plug & Play single photon source



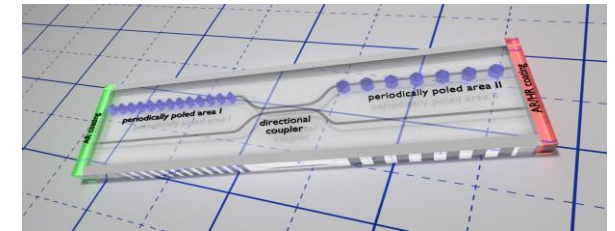
N. Montaut et al, Phys. Rev. Applied **8**, 024021 (2017)

## Integrated N00N source using a non-linear coupler



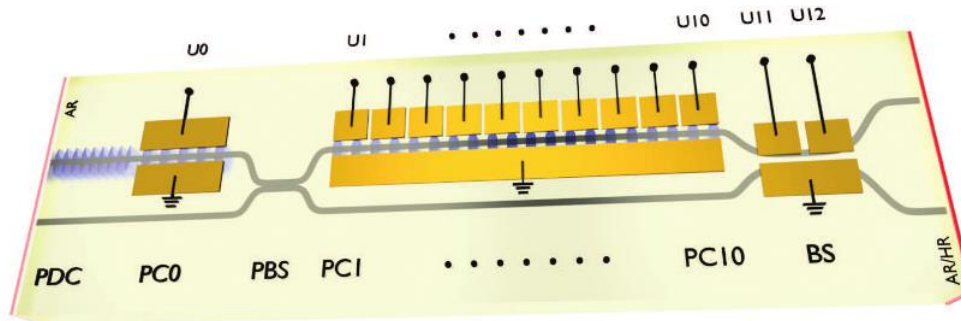
R. Kruse et al, Phys. Rev. A **92**, 053841 (2015)

## Photon triplet generation



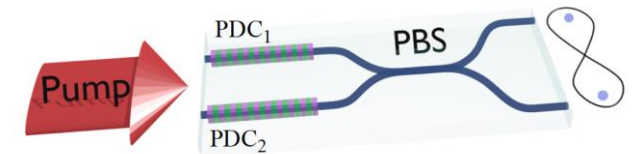
S. Krapick et al, Opt. Exp. **24**, 2836 (2016)

## HOM on a chip



K.-H. Luo et al, Sci. Adv. **5**, eaat1451 (2019)

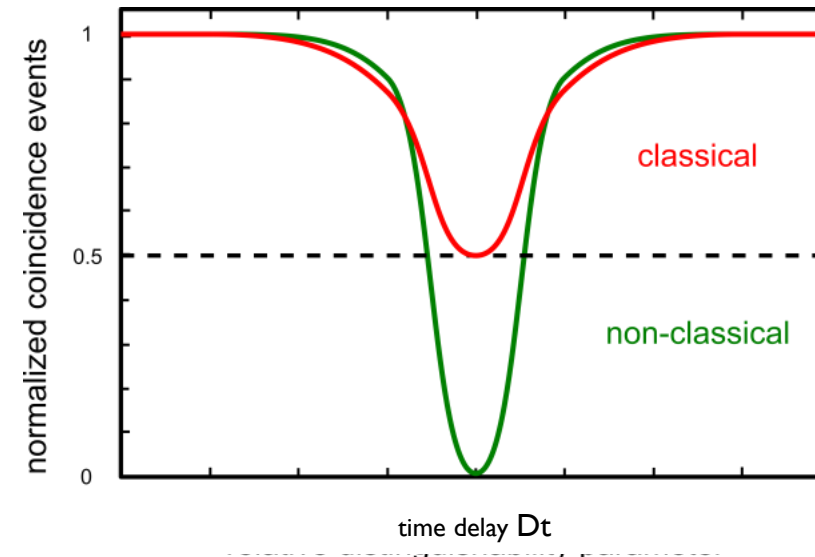
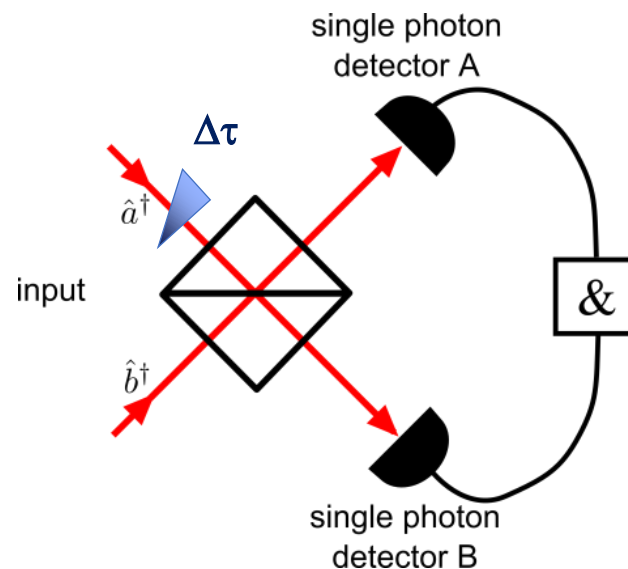
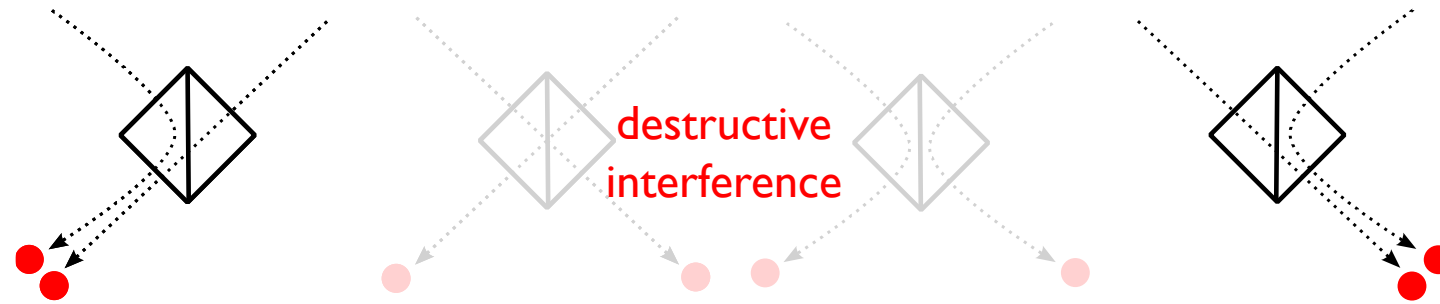
## Polarization entanglement source



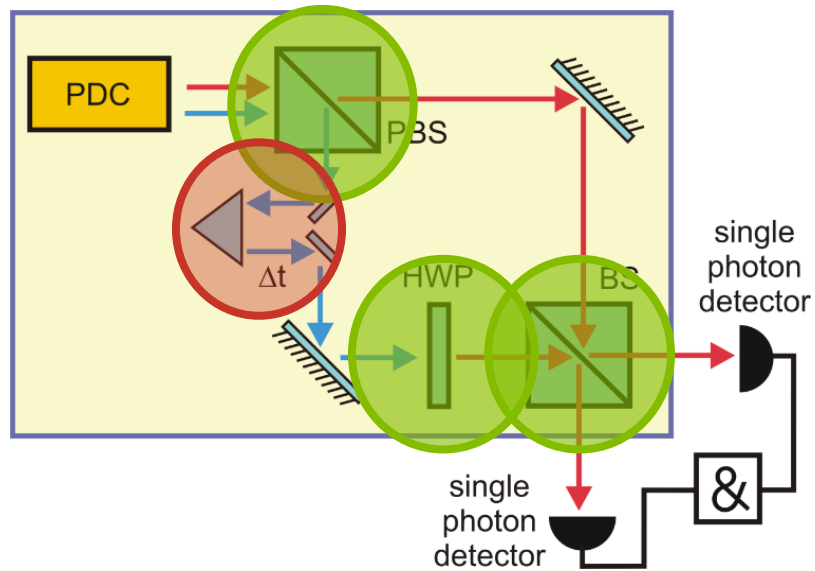
L. Sansoni et al, Quant. Inf. **3**, 5 (2017)

# HOM interference

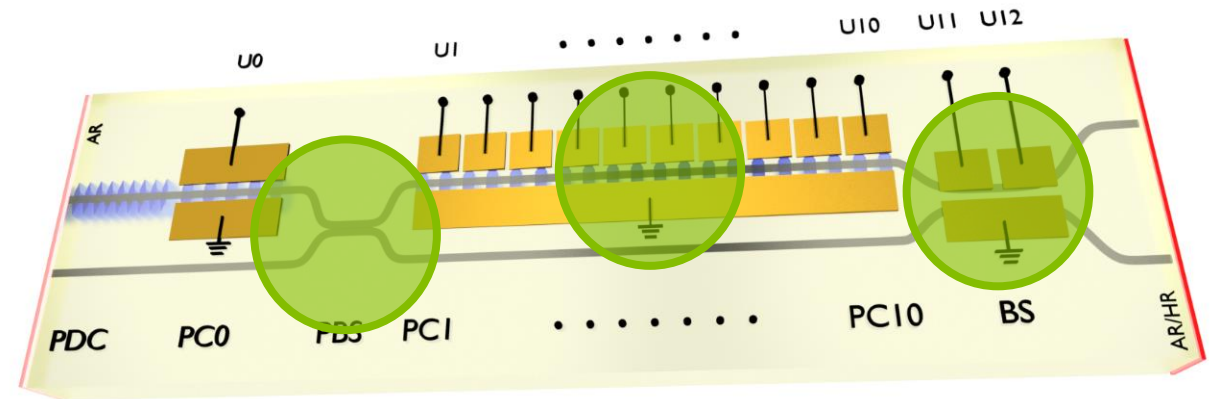
= two-photon interference at balanced (50/50) beamsplitters



Typical bulk optics setup



Our HOM chip

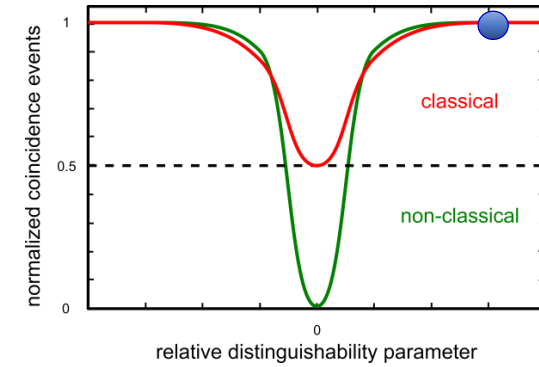
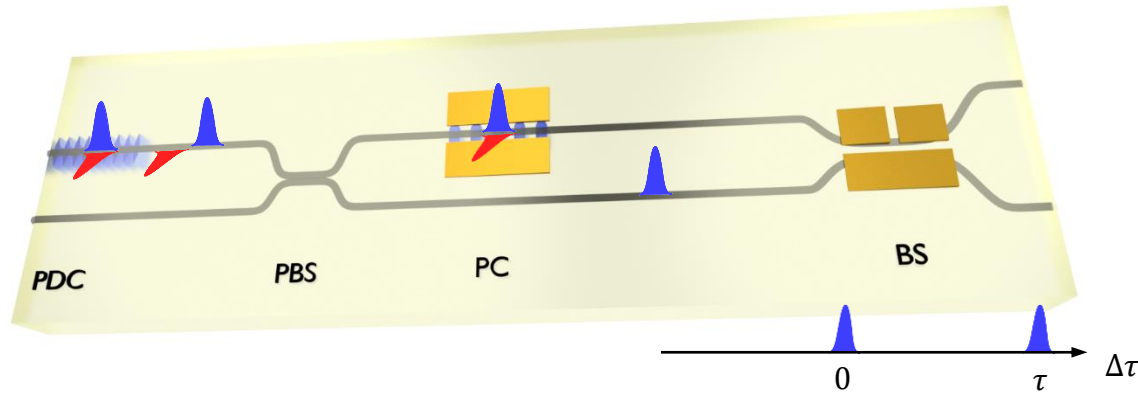


How do we implement a time-delay on chip?



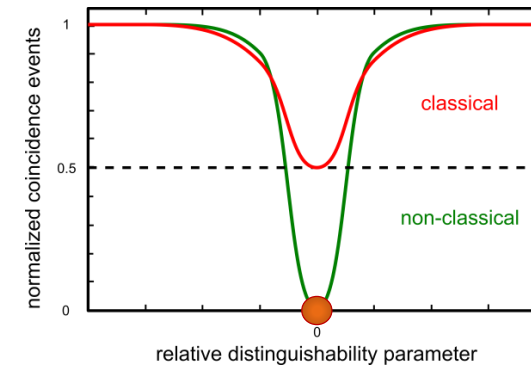
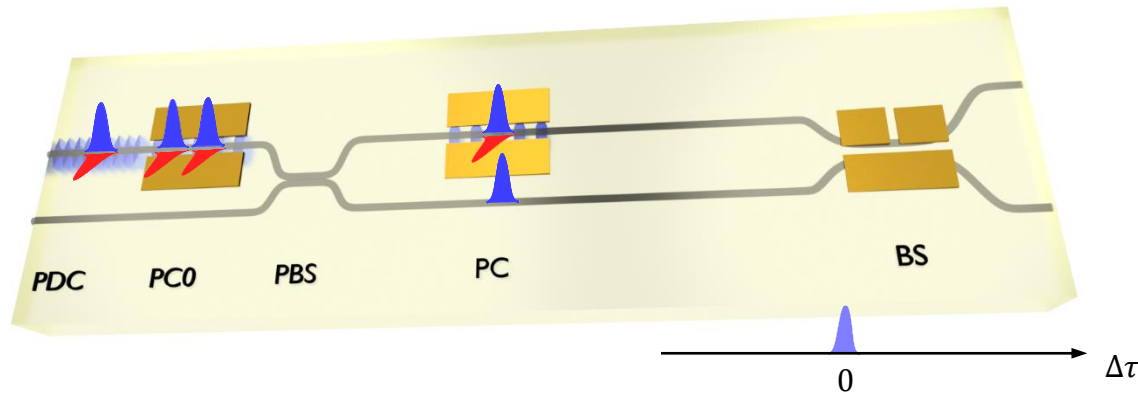
# Birefringence is a friend, not a foe...

$$n_g(\lambda_{s,TE}) \neq n_g(\lambda_{i,TM})$$



# Birefringence is a friend, not a foe...

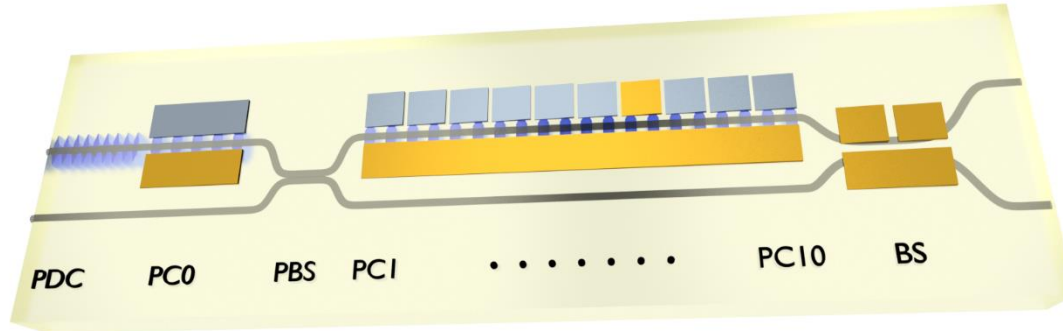
$$n_g(\lambda_{s,TE}) \neq n_g(\lambda_{i,TM})$$



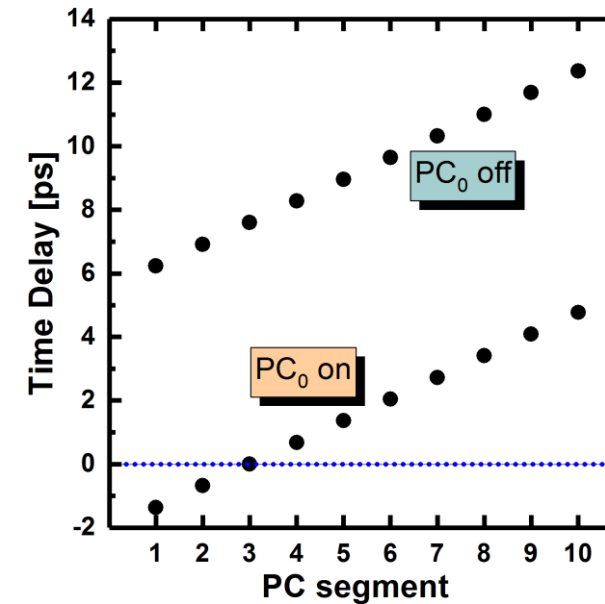
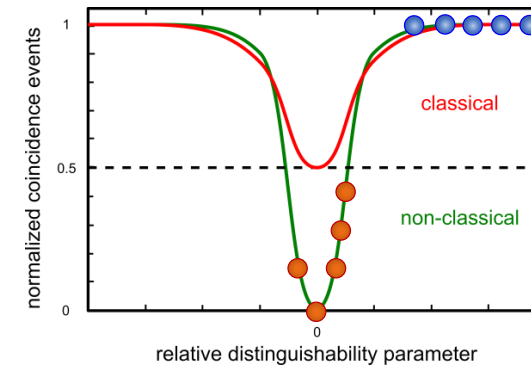
- Additional PC for swapping polarizations to synchronize both photons

# Tuneable on-chip delay

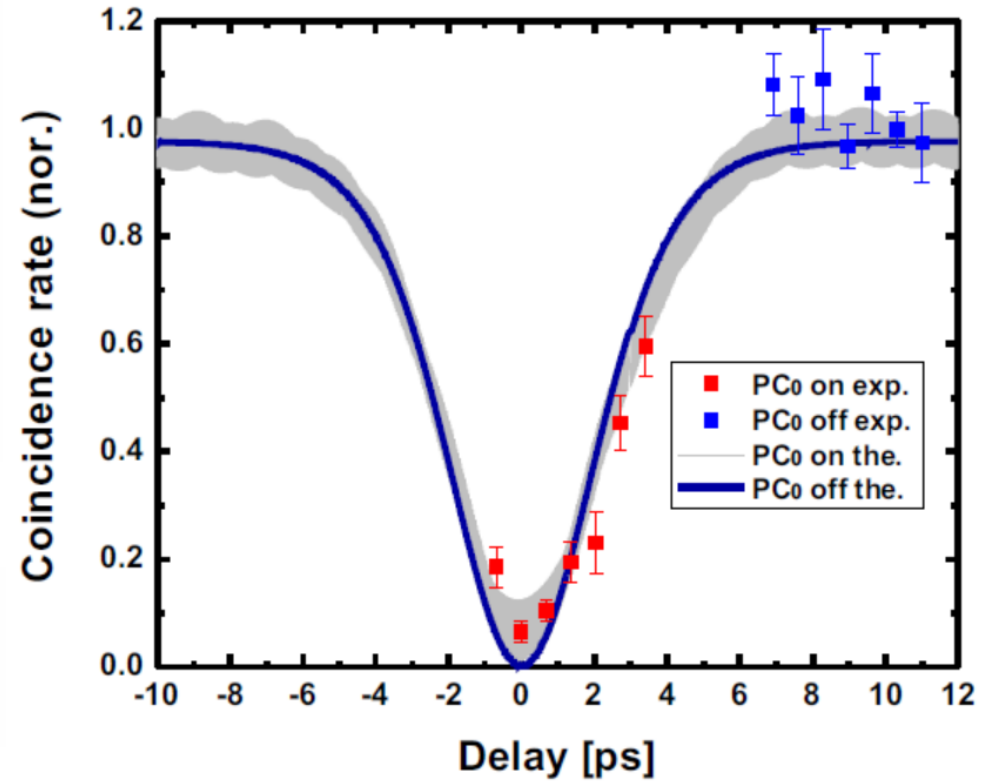
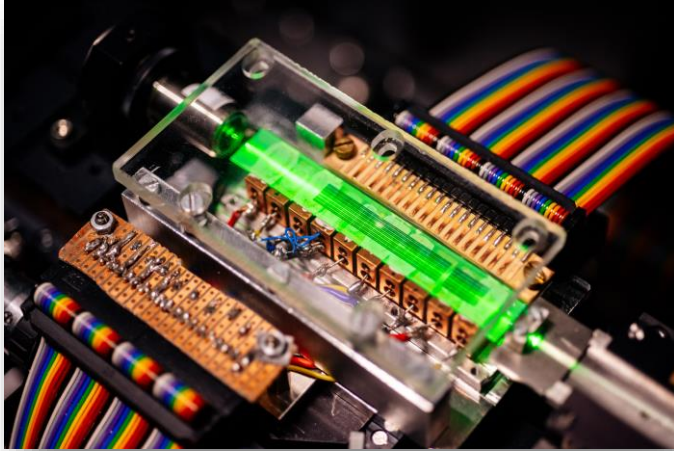
$$n_g(\lambda_{s,TE}) \neq n_g(\lambda_{i,TM})$$



- Additional PC for swapping polarizations to synchronize both photons
- Segmented polarization converters



# HOM on a chip



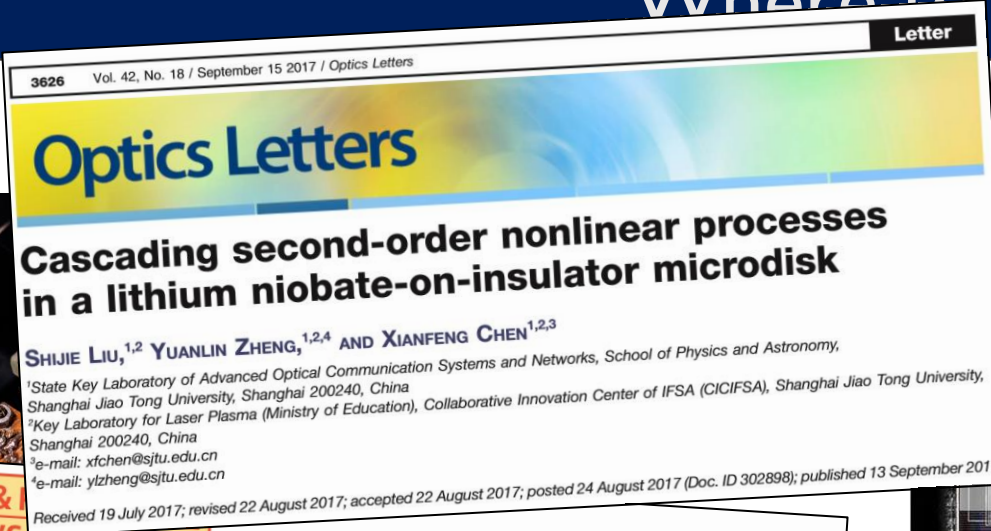
➤ **Tuneable time delay**

$-1 \sim 12 \text{ ps}$

➤ **Dip visibility**

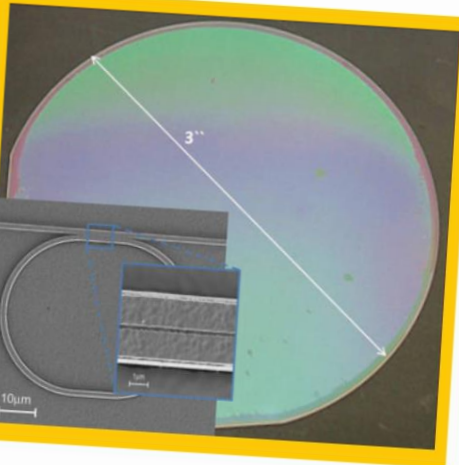
$(93 \pm 2)\%$

# Where to in the future



**LASER & REVIEWS**

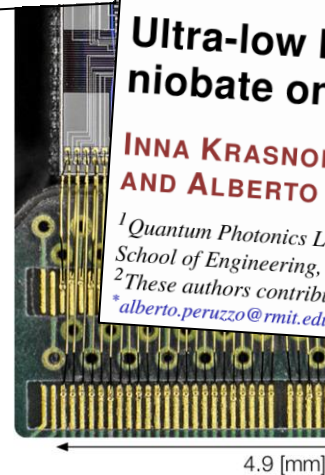
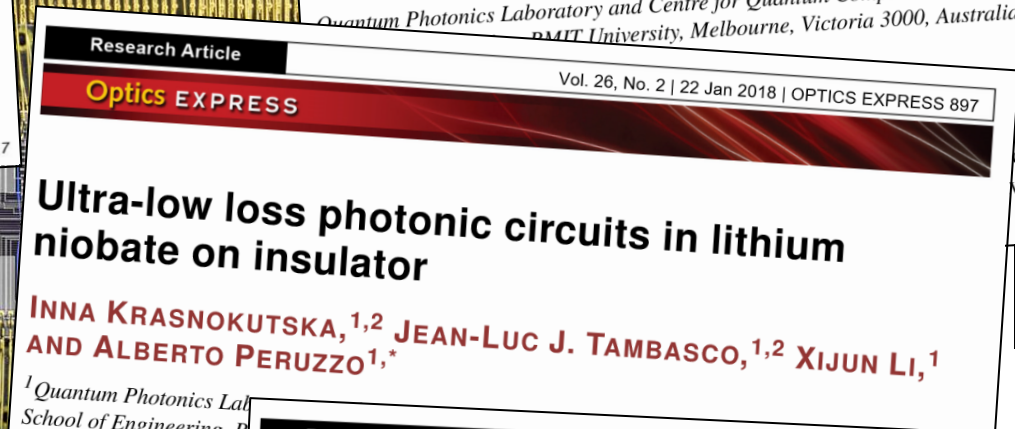
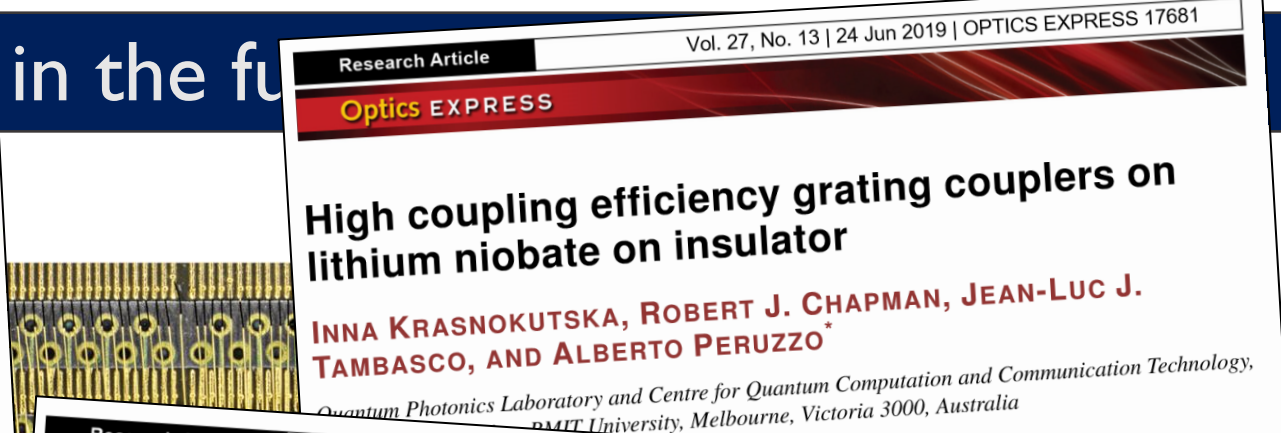
**Abstract** The state-of-the-art of high-refractive-index-contrast single-crystalline thin lithium niobate (LiNbO<sub>3</sub>) films as a new platform for high-density integrated optics is reviewed. Sub-micrometer thin LiNbO<sub>3</sub> films are obtained by "ion-slicing". They can be bonded by two different techniques to a low-index substrate to obtain "lithium niobate on insulator" (LNOI) even as wafer of 3" diameter. Different micro- and nano-structuring techniques have been used to successfully develop micro-photonics devices. To be specific, the fabrication and characterization of LNOI photonic wires with cross-section < 1 μm<sup>2</sup>, periodically poled LNOI photonic wires for second harmonic generation, electro-optically tunable microring resonators, free standing microrings for hybrid integration, and photonic crystal structures are described.



## Lithium niobate on insulator (LNOI) for micro-phonic devices

Gorazd Poberaj<sup>1,3,\*</sup>, Hui Hu<sup>2,4</sup>, Wolfgang Sohler<sup>2</sup>, and Peter Günter<sup>1,5</sup>

Laser Photonics Rev. 6, No. 4, 488–503 (2012) / DOI 10.1002/lpor.201100035



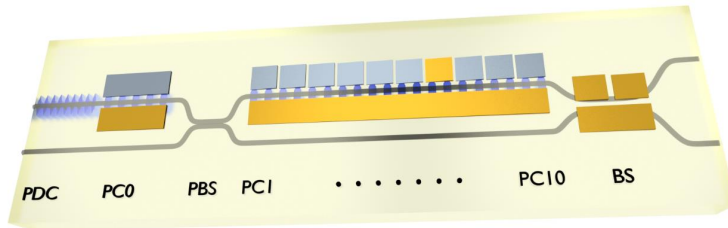
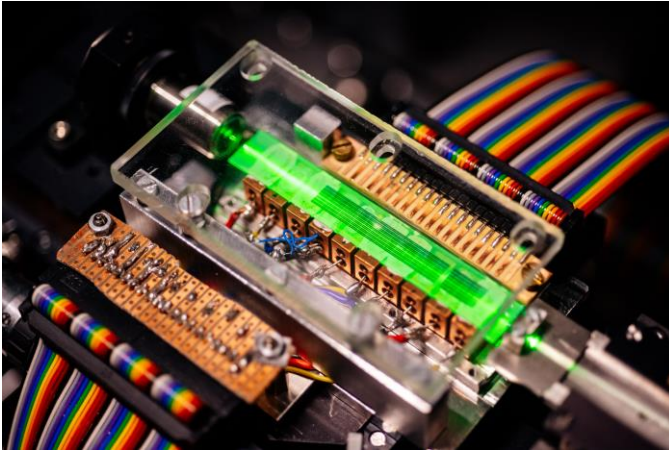
## Silicon photonics integration densit order nonlinearit



C. Harris et al., Optica 5, 1623–1631 (2016)

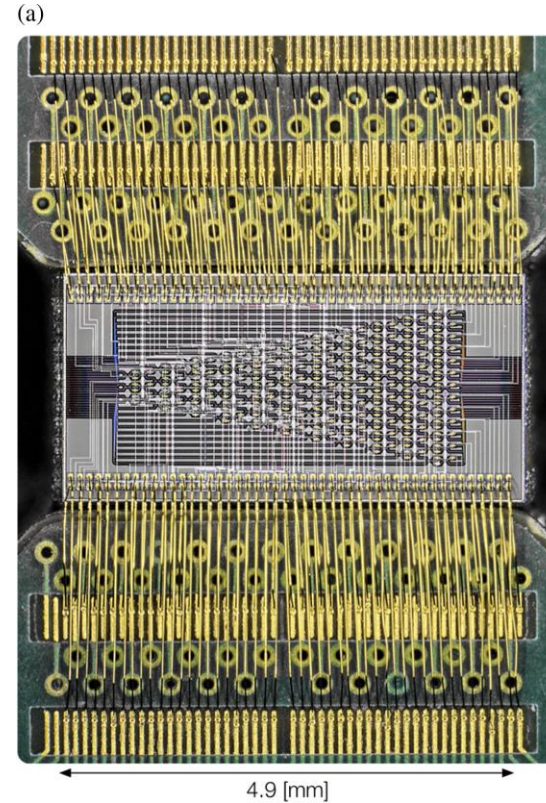


# Where to in the future?



Ti:PPLN circuits have a limited number of components due to the low integration density.

+



= LNOI

Silicon photonics has a huge integration density but no second-order nonlinearity.

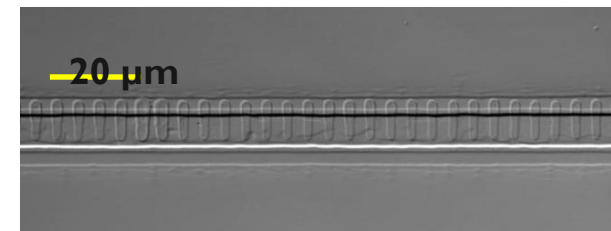
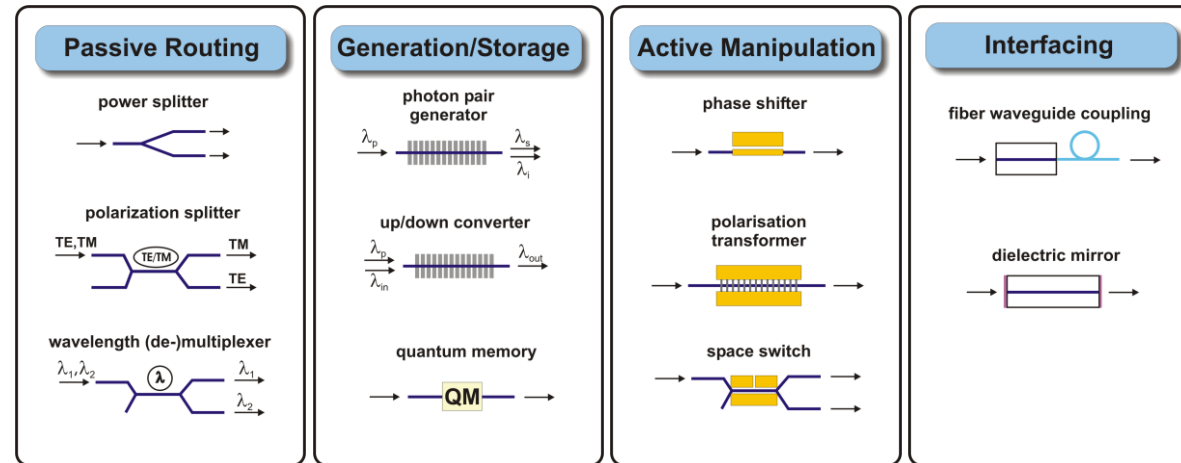
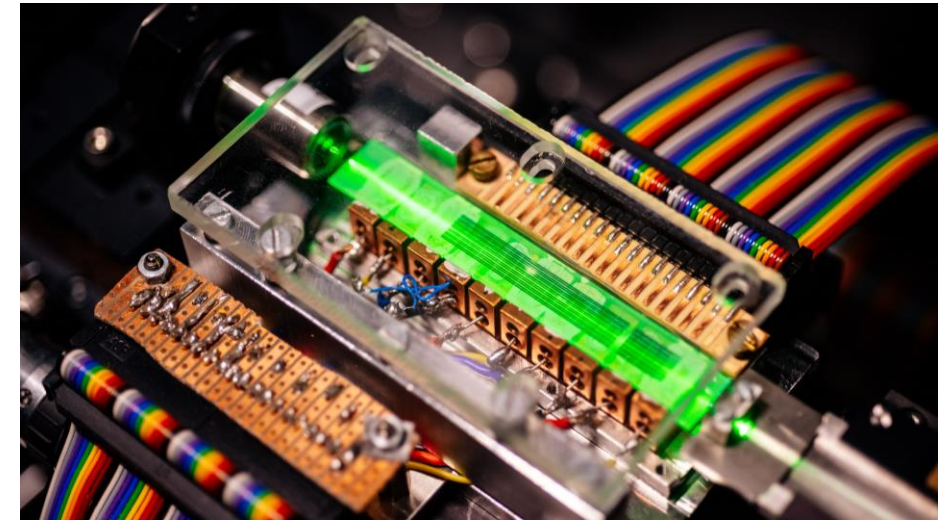
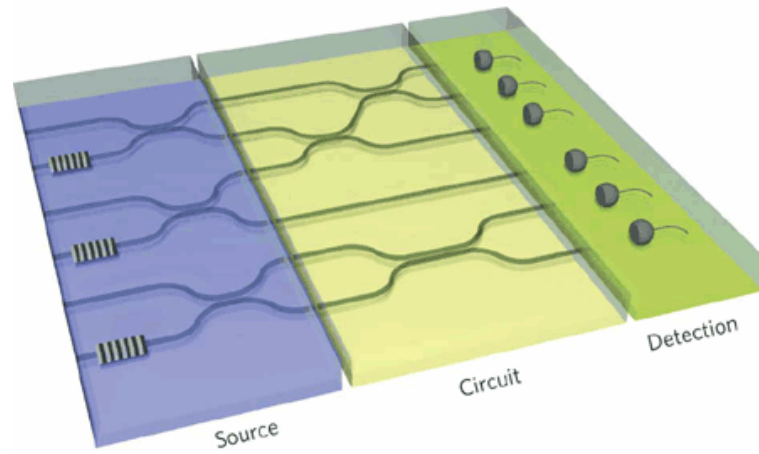
# Summary

Underlying  
concepts

Device  
toolbox

Fabrication  
technology

HOM-on-chip  
circuit





# Thank you for your attention

## Quantum Networks

**Benjamin Brecht**

Sonja Barkhofen

Jan Sperling

Michael Stefszky

Vahid Ansari

Syamsundar De

Thomas Nitsche

Melanie Engelkemeier

Jano Gil Lopez

Johannes Tiedau

Nidhin Prasannan

Rene Pollmann

## Technology

**Christof Eigner**

Laura Padberg

Felix vom Bruch

Viktor Quiring

Raimund Ricken

## Devices

**Harald Herrmann**

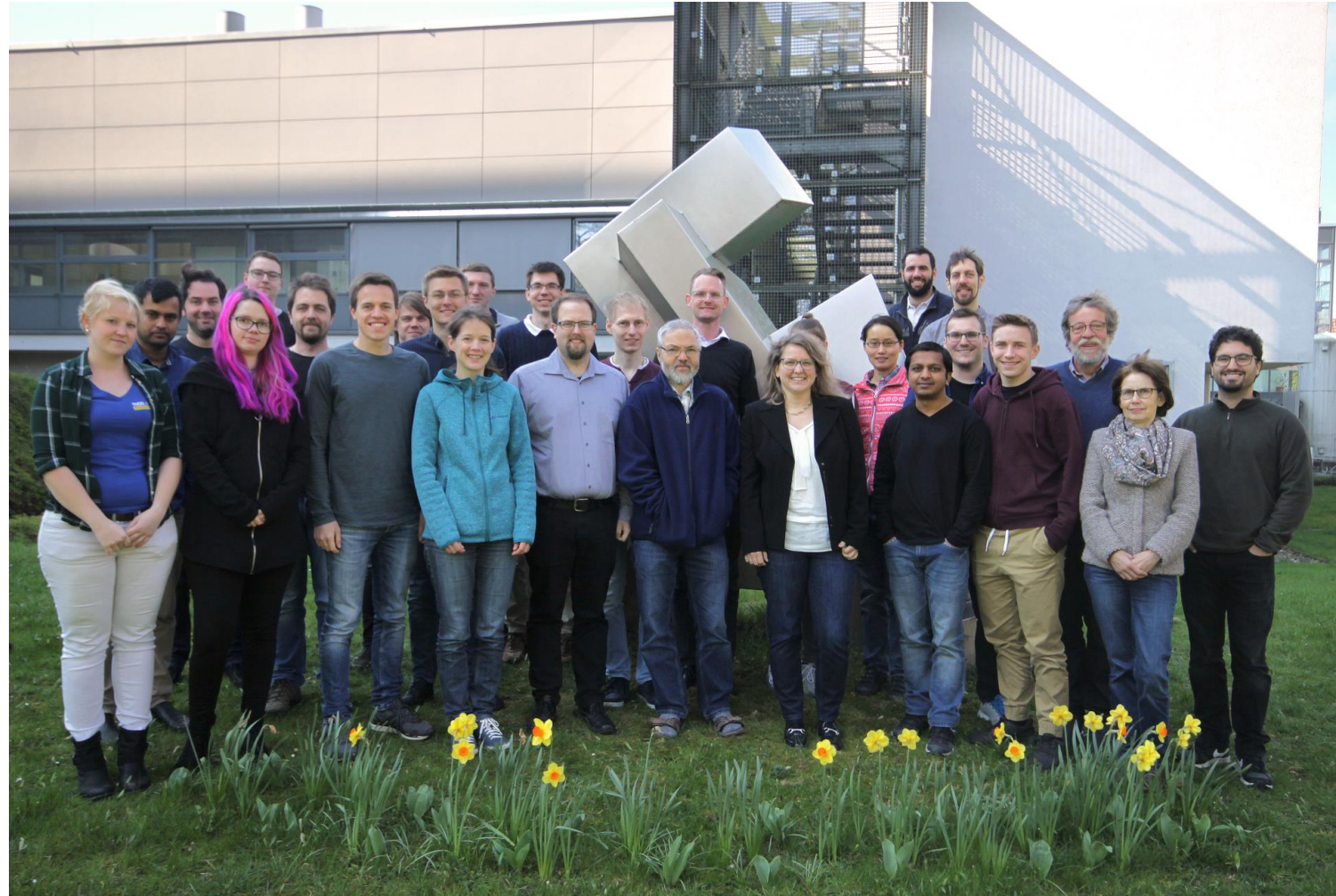
Kai-Hong Luo

Matteo Santandrea

Marcello Massaro

Sebastian Brauner

Christian Kießler



**We have open  
positions  
(and candy...)**



Silberhorn group

